

Ordinal Neural Network Transformation Models: Deep and interpretable regression models for ordinal outcomes

Lucas Kook^{1,2*}, Lisa Herzog^{1,2*}, Torsten Hothorn¹, Oliver Dürr³, Beate Sick^{1,2†}

¹ University of Zurich, Switzerland

² Zurich University of Applied Sciences, Switzerland

³ Konstanz University of Applied Sciences, Germany

Abstract

Outcomes with a natural order, such as quality of life scores or movie ratings, commonly occur in prediction tasks. The available input data are often a mixture of complex inputs like images and tabular predictors. Deep Learning (DL) methods have shown outstanding performances on perceptual tasks. Yet, most DL applications treat ordered outcomes as unordered classes and lack interpretability of individual predictors. In contrast, traditional ordinal regression models are specific for ordered outcomes and enable to interpret predictor effects but are limited to tabular input data. Here, we present the highly modular class of ordinal neural network transformation models (ONTRAMs) which can include both tabular and complex data using multiple neural networks. All neural networks are jointly trained to optimize the likelihood, which is parametrized to take the outcome’s natural order into account. We recapitulate statistical ordinal regression models and discuss how they can be understood as transformation models. Transformation models use a parametric transformation function and a simple distribution, the former of which determines the flexibility and interpretability of the individual model components. We demonstrate how to set up interpretable ONTRAMs with tabular and/or image data. We show that the most flexible ONTRAMs achieve on-par performance with existing DL approaches while outperforming them in training speed. We highlight that ONTRAMs with image and tabular predictors yield correct effect estimates while keeping the high prediction performance of DL methods. We showcase how to interpret individual components of ONTRAMs and discuss the case where the included tabular predictors are correlated with the image data. In this work, we demonstrate how to join the benefits of DL and statistical regression methods to create efficient and interpretable models for ordinal outcomes.

1 Introduction

Many classification problems deal with classes that show a natural order. This includes for example patient outcome scores in clinical studies, quality of life scores for different cities, or quality scores of wine [Burckhardt and Anderson, 2003, Cortez et al., 2009]. These ordinal outcome variables may not only depend on simple, scalar interpretable predictors like age or temperature but also on complex input data such as medical images, networks of public transport, textual descriptions, or

*Authors contributed equally

†Corresponding author, sick@zhaw.ch, beate.sick@uzh.ch

spectra. Depending on the complexity of the input data and the concrete task, different analysis approaches have been established to tackle the ordinal problems.

Ordinal regression as a probabilistic approach has been studied for more than four decades [McCullagh, 1980, Genter and Farewell, 1985]. The goal is to fit an interpretable regression model, which estimates the conditional distribution of an ordinal outcome variable Y based on a set of tabular predictors. The ordinal outcome Y can take values in a set of ordered classes and the tabular predictors are scalar and interpretable like age or blood pressure. Probabilistic ordinal regression models make use of the information contained in the order of the outcome and provide a valid probability distribution instead of a single point estimate for the most likely outcome, which is essential to reflect uncertainty in the predictions. Moreover, the estimated regression parameters are interpretable as the effect a single predictor has on the outcome given the remaining predictors are held constant. This allows experts to assess whether the model corresponds to their field knowledge and provides the necessary trust for application in critical decision making. However, there is a trade-off between interpretability and model complexity. The higher the complexity of a model, the harder it becomes to directly interpret the individual model parameters.

Deep Learning (DL) approaches have gained huge popularity over the last decade and achieved outstanding performances on complex tasks like image-based classification and natural language processing [Goodfellow et al., 2016]. The models take the raw data as input and learn relevant features during the training procedure by transforming the input into a latent representation, which is suitable to solve the task. This avoids the challenging task of feature engineering, which is necessary when working with statistical models. Yet, unlike statistical models, most DL models have a black box character, which makes it hard to interpret individual model components. This is a disadvantage, in particular in fields such as medicine in which the knowledge about the effect of a predictor on the outcome is indispensable. In addition, in a DL approach ordinal outcomes are frequently modeled in the same way as unordered outcomes using multi-class classification (MCC) [e.g., Pratt et al., 2016, Rohrbach et al., 2019]. That is, the softmax function is used as the last layer activation and the neural network is trained by minimizing the categorical cross-entropy loss. In this setting, solely the probability assigned to the observed class is entering the loss function, which ignores the outcome’s natural order and leads to sub-optimal training efficiency as will be shown in this study.

1.1 Our contribution

In this work we introduce ordinal neural network transformation models (ONTRAMs), which unite statistical and deep learning approaches to ordinal regression while conserving the interpretability of classical statistical models and the flexibility of deep learning models. We demonstrate how to combine complex inputs like images with tabular predictors without losing the interpretability of specific model components. We use a theoretically sound maximum likelihood based approach and reparametrize the categorical cross-entropy loss to incorporate the order of the outcome, leading to a more efficient training in case of an ordinal outcome. We view ordinal regression models from a transformation model perspective [Hothorn et al., 2014, Sick et al., 2020]. This change of perspective is useful because it allows a holistic view on regression models, which easily extends beyond the case of ordinal outcomes. In transformation models the problem of estimating a conditional outcome distribution is translated into a problem of estimating the parameters of a monotonically increasing transformation function, which transforms the potentially complex distribution of the outcome to a continuous variable with a predefined, simple distribution F_Z .

The goal of ONTRAMs is to estimate a flexible outcome distribution based on a set of predictors including images and tabular data while keeping components of the model interpretable. In many

applications we face ordinal regression tasks based on imaging and tabular data. Our approach is able to seamlessly integrate both types of data with varyingly complex interactions between the two, by taking a modular approach to model building. The data analyst can choose the scale on which to interpret image and tabular predictors’ effects, such as the odds or hazard scale, by specifying the simple distribution function F_Z . In addition, the user has full control over the complexity of the individual model components. The discussed ONTRAMs will contain at most three (deep) neural networks for the intercepts in the transformation function, the tabular and the image data. Together with the simple distribution function F_Z the output of these three networks (NNs) will be used to evaluate the negative log-likelihood loss. In the end, the neural networks, which control the components of the model, are jointly fit by standard deep learning algorithms based on stochastic gradient descent. In this work, we feature convolutional neural networks (CNNs) for complex input data like images. However, the high modularity of ONTRAMs enables many more applications such as recurrent neural networks (RNNs) for text-based models.

1.2 Organization of this paper

We first describe the necessary theoretical background of multi-class classification and ordinal regression before introducing ordinal neural network transformation models. Afterwards, an outline of related work in the field of deep learning applied to ordinal regression problems is given in Section 2.3. We then provide details about our ONTRAMs in Section 3. Subsequently, we describe the datasets, experiments and models we use to study and benchmark ONTRAMs (Section 4). We end this paper with a discussion of our results and juxtaposition of the different approaches in light of model complexity, interpretability and predictive performance. We provide an appendix with some mathematical details and additional results and address the distinction between ordinal classification and regression.

2 Background

First, we will describe the multi-class classification approach frequently applied in deep learning, which will serve as a baseline model in our experiments. We outline cumulative ordinal regression models as the statistical approach to ordinal regression and how they can be viewed as a special case of transformation models. In the end we summarize related work in the field of deep ordinal regression and interpretable machine learning.

2.1 Multi-class classification

Deep learning models for multi-class classification (MCC) are based on a NN whose output layer contains K units and uses a softmax activation to predict a probability for each class. The softmax activation function is defined as

$$p_k = \text{softmax}(s_k) = \frac{\exp(s_k)}{\sum_{j=1}^K \exp(s_j)}, \quad (1)$$

where s_k is the value of unit k before applying the activation function. Typically, a MCC model is trained by minimizing the categorical cross-entropy loss. The cross-entropy loss is computed over n samples by

$$\text{CE} := - \sum_{i=1}^n \sum_{k=1}^K y_{ki} \log \mathbb{P}(Y = y_{ki} | \mathbf{x}_i) = - \sum_{i=1}^n \log \mathcal{L}_i, \quad (2)$$

with y_{ki} being entry k of the one-hot-encoded outcome for input \mathbf{x}_i , which is one for the observed class and zero otherwise. The probability for the observed class is the likelihood contribution \mathcal{L}_i of the i th observation. It is well known, that the cross-entropy loss is equivalent to the negative log-likelihood for multinomial outcome variables (see Figure 1 A and B). Equation (2) highlights that the likelihood is a local measure, because solely the predicted probability for the observed class contributes to the loss.

2.2 Ordinal regression models

Ordinal regression aims to characterize the whole conditional distribution of an ordinal outcome variable given its predictors. A discussion of ordinal regression and how they can be viewed as transformation models is given in the following.

2.2.1 Cumulative ordinal regression models

The goal of the statistical approach to ordinal regression is mainly to develop an interpretable model for the conditional distribution of the ordered outcome variable Y with K possible values $y_1 < y_2 < \dots < y_K$. Before discussing how interpretable model components are achieved, we discuss the question of how the order of the outcome can be taken into account.

The distribution of an outcome variable is fully determined by its probability density function (PDF). For an ordinal outcome the PDF describes the probabilities of the different classes, which is equivalent to the PDF of an unordered outcome. Yet, unlike an unordered outcome, an ordered outcome possesses a well defined cumulative distribution function (CDF) F_Y , which naturally contains the order. The CDF $F_Y(y_k) = \mathbb{P}(Y \leq y_k)$ is a step function, which takes values between zero and one and describes the probability of an outcome Y of being smaller or equal to a specific class. The steps are positioned at y_k , $k = 1, \dots, K$ and the heights of the steps correspond to the probability $\mathbb{P}(Y = y_k) = F_Y(y_k) - F_Y(y_{k-1}) =: \mathcal{L}_i$ of observing class k (*cf.* Figure 1 A and B). As indicated in the previous subsection, the likelihood contribution for an observation (y_{ki}, \mathbf{x}_i) is given by the predicted probability for the observed class, which can be rewritten as

$$\mathcal{L}_i = \mathbb{P}(Y = y_{ki} | \mathbf{x}_i) = \mathbb{P}(Y \leq y_{ki} | \mathbf{x}_i) - \mathbb{P}(Y \leq y_{(k-1)i} | \mathbf{x}_i), \quad (3)$$

for $k = 1, \dots, K-1$ and $\mathbb{P}(Y \leq y_0) := 0$, $\mathbb{P}(Y \leq y_K) = 1$. Parametrizing the likelihood contributions using the CDF directly enables to incorporate the order of the outcome when formulating regression models for ordinal data (Section 3). It is worth noting that the loss is still the same negative log likelihood as in equation (2) merely using a different parametrization to take the outcome’s natural order into account.

Many ordinal regression models assume the existence of an underlying continuous latent variable (an unobserved quantity) Z . Sometimes, field experts can give an interpretation for the latent variable Z , e.g. the degree of illness of a patient. The ordinal outcome variable Y is understood as a categorized version of Z resulting from incomplete knowledge; we only know the classes in terms of the intervals in which Z lies. Fitting an ordinal regression model based on the latent variable approach aims at finding cut points $h(y_k | \mathbf{x})$ at which Z is separated into the assumed classes (see C in Figure 1). Technically, this is done by setting up a monotonically increasing step function h that transforms the ordinal class values into cut points that retain the order (see Figure 2). Even if Z can not be interpreted directly, using a latent variable approach has advantages, because the chosen distribution of Z determines the interpretability of the terms in the transformation function and the cut points (see section 2.2.2).

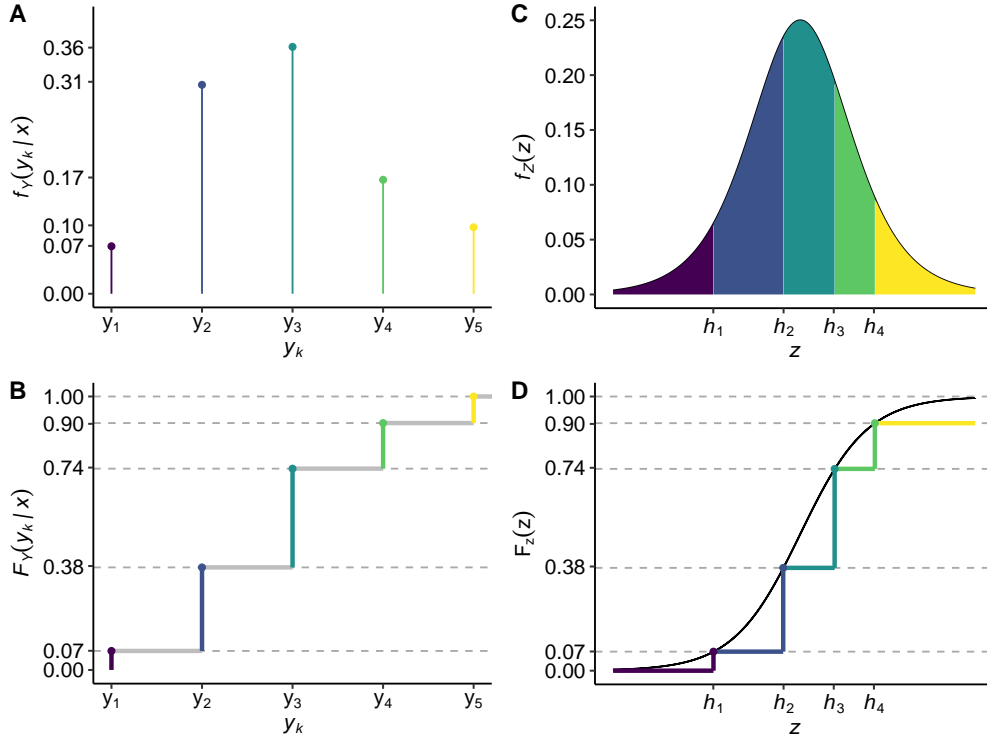


Figure 1: Density and distribution function for an ordered outcome with five classes. (A) The probability density function (PDF) describes the probability of the outcome belonging to class k . (B) The cumulative distribution function (CDF) describes the probability of the outcome belonging to any class below and including class k . The heights of the steps correspond to the probability of belonging to class k , which are given by the PDF. Panels C and D depict the PDF and CDF of the latent variable Z and illustrate the equivalence between modelling on the scale of Y and Z . For brevity the cut points are denoted by $h_k := h(y_k|\mathbf{x})$. Note that $h_5 = +\infty$ gives rise to the yellow area corresponding to the conditional probability of Y belonging to the fifth class, but does not show on the x-axis in panels C and D.

Moreover, the latent variable approach enables to understand ordinal regression as a special case of parametric transformation models, which were recently developed in statistics [Hothorn et al., 2014] and are applicable to a wide range of outcomes [Siegfried and Hothorn, 2020, Buri and Hothorn, 2020] with natural extensions to classical machine learning techniques, such as random forests and boosting [Hothorn and Zeileis, 2017, Hothorn, 2020a]. Transformation models are able to model highly flexible outcome distributions while simultaneously keeping specific model components interpretable. In transformation models the conditional outcome distribution of $(Y|\mathbf{x})$ is modeled by transforming the outcome variable $(Y|\mathbf{x})$ to a variable $(Z|\mathbf{x})$ with known (simple) CDF F_Z , like the Gaussian or logistic distribution. Transformation models in general are thus defined by

$$F_Y(y|\mathbf{x}) = F_Z(h(y|\mathbf{x})), \quad (4)$$

and all models in our proposed framework of ONTRAMs are of this form.

The first step to set up an ordinal transformation model is to choose a continuous distribution for Z , which determines the interpretational scale of the effect of a predictor on the outcome (see Section 2.2.2). The goal is then to fit a monotonically increasing transformation function h ,

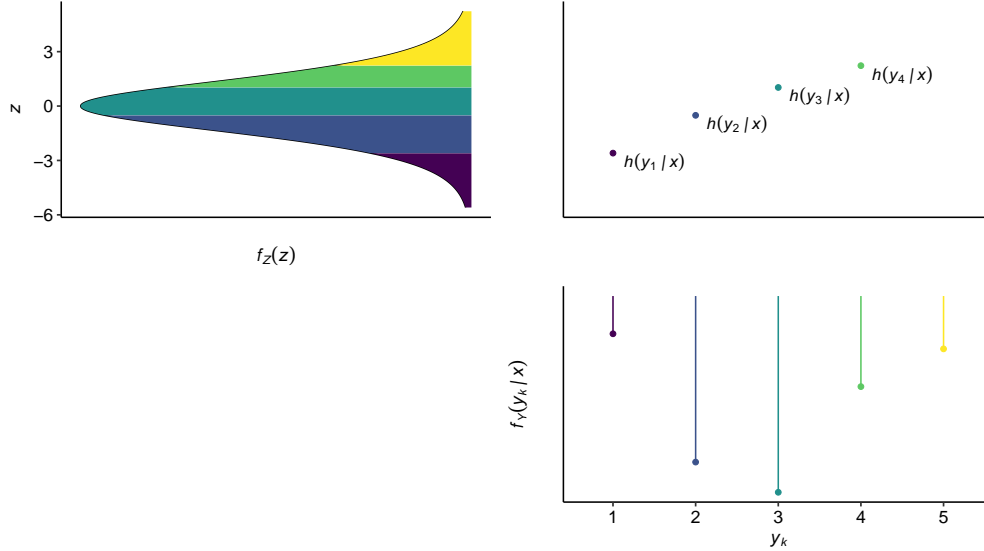


Figure 2: Transformation model likelihoods for a model with ordinal outcome. The lower panel shows the conditional density of Y given \mathbf{x} , which gets mapped onto the density of the latent variable Z (upper left panel) via the transformation function h (upper right panel). The likelihood contributions are in fact probabilities and given by the area under the density of Z between two consecutive cut points in the transformation function. Note that $h(y_5|\mathbf{x}) = +\infty$ does not show on the plot for the transformation function, but is evident from the yellow area under the density of Z .

which maps the observed outcome classes $(y_k|\mathbf{x})$ to the conditional cut points

$$h(y_k|\mathbf{x}), k = 1, \dots, K - 1, \quad (5)$$

of the latent variable Z , as illustrated in Figure 2. In the example in Figure 2 the outcome can take five classes and the $K - 1$ cut points $h(y_1|\mathbf{x})$, $h(y_2|\mathbf{x})$, $h(y_3|\mathbf{x})$, and $h(y_4|\mathbf{x})$ have to be estimated. The first class of Y on the scale of Z is given by the interval $(-\infty, h(y_1|\mathbf{x})]$, the fifth class as $(h(y_4|\mathbf{x}), +\infty)$, so often the conventions $h(y_0|\mathbf{x}) = -\infty$ and $h(y_K|\mathbf{x}) = +\infty$ are used. The likelihood contribution of a given observation (y_{ki}, \mathbf{x}_i) can now be derived from the CDF of Z instead of Y and is given by

$$\begin{aligned} \mathcal{L}_i(h; y_{ki}, \mathbf{x}_i) &= \mathbb{P}(Y = y_{ki}|\mathbf{x}_i) \\ &= F_Y(y_{ki}|\mathbf{x}_i) - F_Y(y_{(k-1)i}|\mathbf{x}_i) \\ &= F_Z(h(y_{ki}|\mathbf{x}_i)) - F_Z(h(y_{(k-1)i}|\mathbf{x}_i)). \end{aligned} \quad (6)$$

The single likelihood contributions are the heights of the steps in the CDF or equivalently the area under the density of the latent variable Z between two consecutive cut points (cf. Figure 2, panels on the right). Note that two consecutive cut points enter the likelihood, such that the natural order of the outcome is used to parametrize the likelihood, although a likelihood contribution is given by the probability of the observed class alone. Consequently, minimizing the negative log-likelihood

$$-\ell(h; y_{1:n}, \mathbf{x}_{1:n}) = -\sum_{i=1}^n \log \mathcal{L}_i(h; y_i, \mathbf{x}_i) \quad (7)$$

estimates the conditional outcome distribution of $(Y|\mathbf{x})$ by estimating the unknown parameters of the transformation function, which in our application are the cut points of Z . Note that in principle this formulation allows us to directly incorporate uncertain observations, for instance, an observation may lie somewhere in $[y_k, y_{k+2}]$, $k \leq K - 2$ if a rater is uncertain about the quality of a wine or a patient rates their pain in between two classes.

2.2.2 Interpretability in proportional odds models

The interpretability of a transformation model depends on the choice of the distribution F_Z of the latent variable Z and the transformation function h . A summary of common interpretational scales is given in Appendix B.

Here, we demonstrate interpretability through the example of a proportional odds model, which is well known in statistics [Tutz, 2011]. For the distribution of Z we choose the standard logistic distribution (denoted by F_L), whose CDF is given by $F_Z(z) = F_L(z) := (1 + \exp(-z))^{-1}$. The transformation function h is parametrized as

$$h(y_k|\mathbf{x}) = \vartheta_k - \sum_{j=1}^J \beta_j x_j = \vartheta_k - \mathbf{x}^\top \boldsymbol{\beta}, \quad j = 1, \dots, J. \quad (8)$$

A transformation model with such a transformation function is called linear shift model, since a change Δx_j in a single predictor x_j causes a linear shift of size $\beta_j \Delta x_j$ in the transformation function. In Figure 3 this is visualized for an outcome y_k depending on a single predictor x , which is increased by one unit (here from 0 to 1). This increase results in a simple shift of size β in the transformation function (Figure 3, middle panel). However, the resulting conditional distribution changes in a more complex way (Figure 3, left panel). Note that the shape of the transformation function h does not depend on x and stays unchanged while it is shifted downwards. The popularity of this transformation model with $F_Z = F_L$ is due to the insightful interpretation of the parameter β_j as demonstrated in the following.

Based on the simple distribution F_Z and the transformation function h , the odds for the outcome to belong to a class higher than class y_k can be written as

$$\begin{aligned} \text{odds}(Y > y_k|\mathbf{x}) &= \frac{\mathbb{P}(Y > y_k|\mathbf{x})}{\mathbb{P}(Y \leq y_k|\mathbf{x})} = \frac{1 - F_Y(y_k|\mathbf{x})}{F_Y(y_k|\mathbf{x})} \\ &= \frac{1 - F_Z(h(y_k|\mathbf{x}))}{F_Z(h(y_k|\mathbf{x}))} = \frac{1 - F_L(\vartheta_k - \mathbf{x}^\top \boldsymbol{\beta})}{F_L(\vartheta_k - \mathbf{x}^\top \boldsymbol{\beta})}. \end{aligned} \quad (9)$$

When increasing the predictor x_j by one unit and holding all other predictors constant we change the vector \mathbf{x} to \mathbf{x}' and obtain, after some basic mathematical transformation (*cf.* Appendix B),

$$\begin{aligned} \text{odds}(Y > y_k|\mathbf{x}') &= \frac{1 - F_L(\vartheta_k - \mathbf{x}'^\top \boldsymbol{\beta})}{F_L(\vartheta_k - \mathbf{x}'^\top \boldsymbol{\beta})} = \frac{1 - F_L(\vartheta_k - \mathbf{x}^\top \boldsymbol{\beta} - \beta_j)}{F_L(\vartheta_k - \mathbf{x}^\top \boldsymbol{\beta} - \beta_j)} \\ &= \text{odds}(Y > y_k|\mathbf{x}) \cdot \exp(\beta_j). \end{aligned} \quad (10)$$

Note that the odds change by a constant factor $\exp(\beta_j)$ independent of k . Hence, the parameter β_j in the linear shift term can be interpreted as the log-odds ratio of the outcome belonging to a higher outcome class than y_k , when increasing the predictor x_j by one unit and holding the remaining predictors constant

$$\log \text{OR}_{\mathbf{x} \rightarrow \mathbf{x}'} = \log \left(\frac{\text{odds}(Y > y_k|\mathbf{x}')}{\text{odds}(Y > y_k|\mathbf{x})} \right) = \beta_j. \quad (11)$$

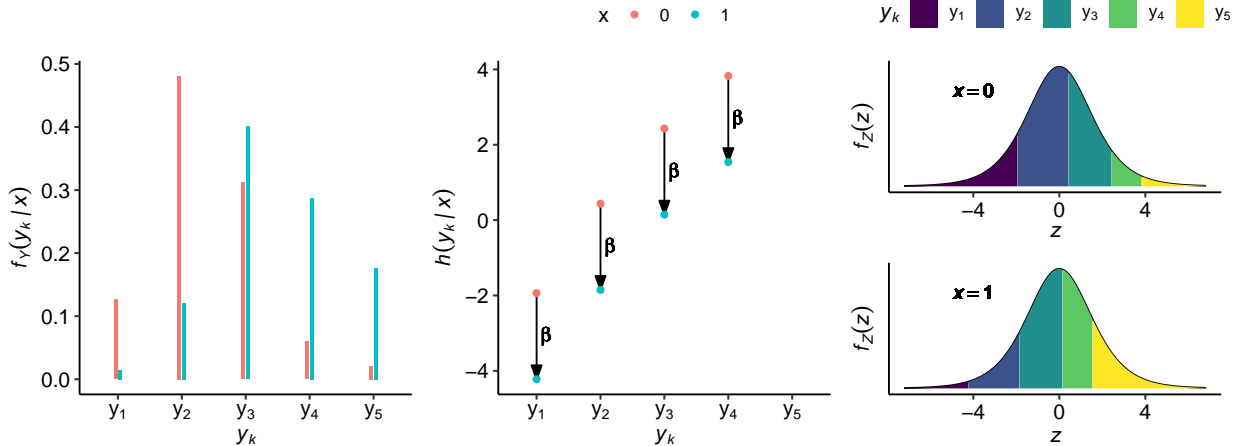


Figure 3: The conditional probability density, transformation function and latent representation of the ordinal outcome Y with 5 classes depending on a single predictor x which is increased by $\Delta x = 1$ from 0 to 1. The density of $(Y|x)$ for $x = 0$ and $x = 1$ is shown in the left panel. The simple linear shift model (see eq. (8)) imposes a downward shift of the transformation function by β when increasing the predictor from $x = 0$ to $x = 1$ (middle panel). The shift in the transformation function translates into a shift in the conditional cut points $h(y_k|x)$ under the density of the latent variable Z (right panel). Shifting the transformation function downwards results in higher probabilities of Y belonging to a higher class.

This is depicted in Figure 3 for a positive valued β , where the effect of increasing the corresponding feature by one unit increases the odds for the outcome to belong to a higher class. More specific, the odds of the outcome for a higher class than y_k is increased by a factor $\exp(\beta_j)$ which holds for each y_k . Because the effect of β is the same for each class boundary these models are referred to as proportional odds models [Tutz, 2011].

2.3 Related work

Ordinal regression models, in multiple variants, have been studied in machine learning as extensions of different popular methods like Gaussian Processes [Chu and Ghahramani, 2005], support vector machines [Cardoso and Costa, 2007, Chu and Keerthi, 2007], boosting [Hothorn et al., 2010], and neural networks [Cardoso and Costa, 2007], and are conveniently available in software packages like **ORCA** for Matlab [Sánchez-Monedero et al., 2019] and **ordinal** [Christensen, 2019] for R. Consequently, ordinal regression is studied in the context of deep learning as well.

Vargas et al. [2020] concisely summarize recent approaches to tackle ordinal regression and classification problems with deep learning methods, which range from using an ordinal metric for the evaluation of multi-class classification models to the construction of novel ordinal loss functions. The earliest approaches used the equivalence of an ordinal regression problem with outcome $Y \in \{y_1 < \dots < y_K\}$, to the $K - 1$ binary sub-problems given by $\mathbb{1}(Y \leq y_k)$, $k = 1, \dots, K$ [Frank and Hall, 2001], which is still being used in applications such as age estimation [Niu et al., 2016, Zhu et al., 2018]. Amorim et al. [2018] comment on the limited interpretability of the ensemble of neural networks in this K -rank approach. Later, Cheng et al. [2008] devised a cumulative dummy encoding for the ordinal response where for $Y = y_k$ we have $y_i = 1$ if $i \leq k$ and 0 otherwise. Cheng and

colleagues then suggest a sigmoid activation for the last layer of dimension K , together with two loss functions (relative entropy and a squared error loss), which remains highly popular in applications [Liu et al., 2017, Garg and Manwani, 2019, Cao et al., 2019, Zhu et al., 2020]. In the meantime the focus shifted towards novel ordinal loss functions involving Cohen’s kappa [de La Torre et al., 2018, 2020, Vargas et al., 2019, 2020], which is described in more detail in Appendix C. Liu et al. [2019] took a probabilistic approach using Gaussian processes with an ordinal likelihood similar to the cumulative probit model (cumulative ordinal model with $F_Z = \Phi$).

Deep transformation models have very recently been applied to regression problems with a continuous outcome [Sick et al., 2020]. Here, the authors parametrized the transformation function as a composition of linear and sigmoid transformations and a flexible basis expansion that ensures monotonicity of the resulting transformation function. The authors applied deep transformation models to a multitude of benchmark datasets with a continuous outcome and demonstrated a performance that was comparable to or better than other state of the art models. However, in one of the benchmark dataset the authors treated a truly ordinal outcome as continuous, as done by all the other benchmark models. This is indicative for the lack of deep learning models for ordered categorical regression.

In general, deep learning models suffer from a lack of interpretability of the predictions they make [Goodfellow et al., 2016]. A recent approach to overcome this lack of interpretability is to build surrogate models on top of the black-box model’s predictions, which are easier to interpret. One such model is LIME [Ribeiro et al., 2016]. In the present work we take a different approach to interpretability rooted in statistical regression models, where the interpretability of individual input features is determined by the explicit structure of the transformation function. Agarwal et al. [2020] take the same approach in the framework of generalized additive models [GAMs, e.g., Hastie and Tibshirani, 1990].

3 Ordinal neural network transformation models

Here, we present ordinal neural network transformation models, which unite cumulative ordinal regression models with deep neural networks and seamlessly integrate complex data like images (\mathbf{B}) and/or tabular data (\mathbf{x}). At the heart of an ONTRAM lies a parametric transformation function $h(y_k|\mathbf{x}, \mathbf{B})$ which transforms the ordinal outcome y_k to cut points of a continuous latent variable and controls the interpretability and flexibility of the model (*cf.* Figure 2). The ordering of the outcome is incorporated in the ONTRAM loss function by defining it via the cumulative distribution function

$$\text{NLL} := -\frac{1}{n} \sum_{i=1}^n \log (F_Z(h(y_{ki}|\mathbf{x}_i, \mathbf{B}_i)) - F_Z(h(y_{(k-1)i}|\mathbf{x}_i, \mathbf{B}_i))). \quad (12)$$

In the following we describe the terms of the parametric transformation function and their interpretability. The parameters of these terms are controlled by NNs, which are jointly fitted in an end-to-end fashion by minimizing the NLL.

Modularity: We view ONTRAMs as a special case of transformation models and characterize them through their transformation function $h(y_k|\mathbf{x}, \mathbf{B})$, which determines the complexity and, together with F_Z , the interpretability of an ONTRAM. The transformation function consists of an intercept term, optionally followed by additive shift terms, which depend in a more or less complex manner on different input data.

The intercept term controls the shape of the transformation function:

1. Simple intercepts (SI) ϑ_k , $k = 1, \dots, K - 1$ are unconditional, i.e. the shape of the transformation function is independent of the input data. SIs can be modeled as a single layer neural network with $K - 1$ output units and linear activation function. The input is given by 1. The outputs are given by $\gamma_1, \dots, \gamma_{K-1}$ controlling the intercepts (see upper left panel in Figure 4).
2. Complex intercepts (CI), on the other hand, depend on the input data, which may be tabular data, image data or a combination of both, yielding $\vartheta_k(\mathbf{x})$, $\vartheta_k(\mathbf{B})$, or $\vartheta_k(\mathbf{x}, \mathbf{B})$, respectively. CIs enable more complex transformation functions, whose shape may vary with the input. Depending on the type of input data, CIs are modeled using a multi-layer fully connected neural network, a convolutional neural network or a combination of both. Analogous to SI terms, the number of output units in the last layer is equal to $K - 1$ with linear activation function, yielding $\gamma_1(\mathbf{x}, \mathbf{B}), \dots, \gamma_{K-1}(\mathbf{x}, \mathbf{B})$ depending on the input (see upper right panel in Figure 4).

To ensure that the transformation function is non-decreasing, the outputs $\gamma_1, \dots, \gamma_{K-1}$ of simple and complex intercept models are transformed before entering the likelihood via

$$\vartheta_k = \vartheta_1 + \sum_{i=2}^k \exp(\gamma_i), \quad k = 2, \dots, K - 1, \quad (13)$$

$$\vartheta_0 = -\infty, \vartheta_1 = \gamma_1, \vartheta_K = +\infty.$$

The addition of $\vartheta_0 = -\infty$ and $\vartheta_K = +\infty$ is important for computing the loss as described in Section 2. Enforcing a monotone increasing transformation function via eq. (13), such that $\vartheta_0 < \vartheta_1 \leq \dots < \vartheta_K$, has been done similarly in the literature. In what Cheng et al. [2008] call threshold models, γ_i is squared instead of taking the exponential to ensure the intercept function is non-decreasing [Liu et al., 2019, Vargas et al., 2020]. Note that the special case $\vartheta_k(\mathbf{x}, \mathbf{B})$ already includes both tabular and image data. That is, the transformation function and therefore the outcome distribution is allowed to change with each input \mathbf{x} and \mathbf{B} , which represents the most flexible model possible. In fact, this most flexible ONTRAM is equivalent to using softmax as the last layer activation function and a categorical cross-entropy loss, albeit parametrized differently to take the order of the outcome into account.

Shift terms impose data dependent vertical shifts on the transformation function:

1. Linear shift (LS) terms $\mathbf{x}^\top \boldsymbol{\beta}$ are used for tabular features and are directly interpretable (see Section 2.2.2). The components of the parameter $\boldsymbol{\beta}$ can be modeled as the weights of a single layer neural network with input \mathbf{x} , one output unit with linear activation function and without a bias term (see lower left panel in Figure 4).
2. Complex shift (CS) terms depend on tabular predictors or image data. Complex shift terms are modeled using flexible dense and/or convolutional NNs with input \mathbf{x} and/or \mathbf{B} , and a single output unit with linear activation (see lower right panel in Figure 4). Similar to linear shift terms, the output of β and η can be interpreted as the log odds of belonging to a higher class, compared to all lower classes, if $F_Z = F_L$. Again, this effect is common to all class boundaries. In contrast to a linear shift term, we can model a complex shift for each tabular predictor $\beta(x_j)$ akin to a generalized additive model. Alternatively, we can model a single complex shift $\beta(\mathbf{x})$ for all predictors, which allows for higher order interactions between the predictors. This way, the interpretation of an effect of a single predictor is lost in favour of higher model complexity.

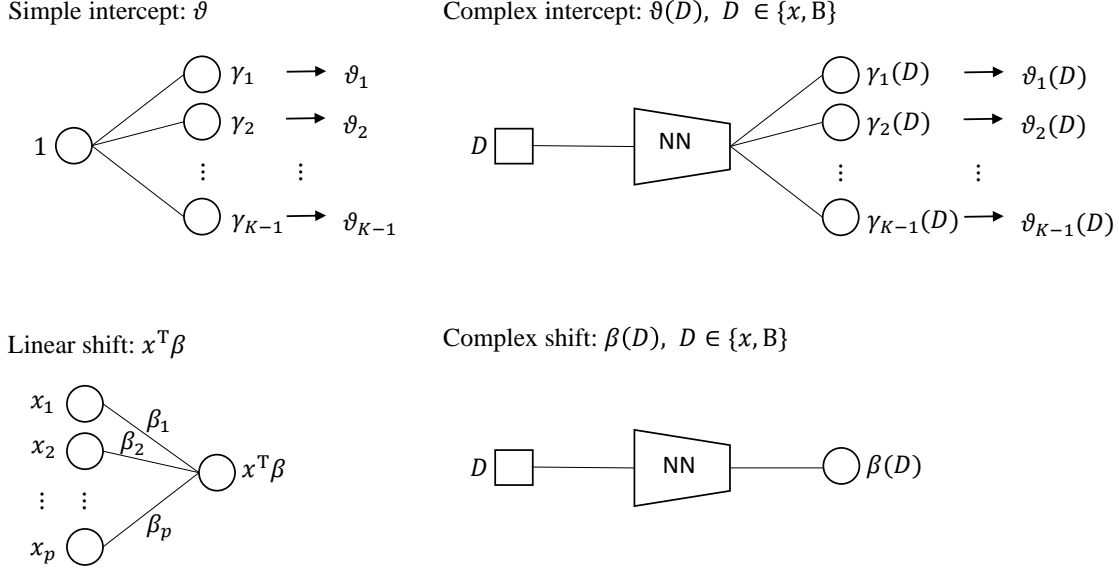


Figure 4: Architecture building blocks of ONTRAMs. Simple intercept and linear shift terms are modeled using a single-layer neural network. Complex intercept and complex shift terms are allowed to depend on the input data in a more complex manner. The shape of the outputs are fix but the input data D can be a single tabular predictor x_j or a set of tabular predictors \mathbf{x} or images \mathbf{B} . The NN may be any neural network to solve the task at hand, which, for instance, may be a fully connected or a convolutional neural network.

Interpretability and flexibility: In the following, we will present a non-exhaustive collection of ONTRAMs integrating both tabular and image data. We start to introduce the least complex model with the highest degree of interpretability and end with the most complex model with the lowest degree of interpretability.

The simplest ONTRAM conditioning on tabular data \mathbf{x} and image data \mathbf{B} is given by

$$h(y_k|\mathbf{x}, \mathbf{B}) = \vartheta_k - \mathbf{x}^\top \boldsymbol{\beta} - \eta(\mathbf{B}), \quad (14)$$

where ϑ_k is a simple intercept corresponding to class k , $\boldsymbol{\beta}$ is the weight vector of a single layer NN as described above and $\eta(\mathbf{B})$ the output of a CNN (Figure 4, panel A). The above model can be made more flexible, yet less interpretable, by substituting the linear predictor for a more complex neural network β , such that

$$h(y_k|\mathbf{x}, \mathbf{B}) = \vartheta_k - \beta(\mathbf{x}) - \eta(\mathbf{B}), \quad (15)$$

where $\beta(\mathbf{x})$ is now a log odds ratio function that allows for higher order interactions between all predictors in \mathbf{x} . For instance, one may be interested in the odds ratio $\text{OR}_{\mathbf{B} \rightarrow \mathbf{B}'}$ of belonging to a higher category when changing an image \mathbf{B} to \mathbf{B}' and holding all other variables constant. As a special case, complex shifts include an additive model formulation in the spirit of generalized additive models (GAMs) by explicitly parametrizing the effect of each predictor x_j with a single neural network β_j [Hastie and Tibshirani, 1990, Agarwal et al., 2020]

$$h(y_k|\mathbf{x}, \mathbf{B}) = \vartheta_k - \sum_{j=1}^J \beta_j(x_j) - \eta(\mathbf{B}), \quad j = 1, \dots, J. \quad (16)$$

For $F_Z = F_L$ the complex shift term $\beta_j(x)$ can be interpreted as a log-odds ratio for the outcome to belong to a higher class than y_k compared to the scenario where $\beta_j(x) = 0$, all other predictors kept constant.

Another layer of complexity can be added by allowing the intercept function ϑ_k for $Y = y_k$, to depend on the image

$$h(y_k|\mathbf{x}, \mathbf{B}) = \vartheta_k(\mathbf{B}) - \beta(\mathbf{x}). \quad (17)$$

In this transformation function we call $\vartheta_k(\mathbf{B})$ complex intercept, because the intercept function is allowed to change with the image (Figure 4 B). One does not necessarily have to stop here. Including both the image and the tabular data in a complex intercept

$$h(y_k|\mathbf{x}, \mathbf{B}) = \vartheta_k(\mathbf{x}, \mathbf{B}) \quad (18)$$

represents the most flexible model whose likelihood is equivalent to the one used in MCC models, solely with a different parametrization.

Computational details: The parameters of an ONTRAM are jointly trained via back-propagation. The parameters enter the loss function via the outputs of the simple/complex intercept and shift terms modeled as neural networks (see Figure 4). The gradient of the loss with respect to all trainable parameters is computed via automatic differentiation in the `TensorFlow` framework and used to update the weights via stochastic gradient descent. Note that any pre-implemented optimizer can be used and that there are no constraints on the architecture of the individual components besides their last-layer dimension and activation.

4 Experiments

We perform several experiments on data with an ordinal outcome to evaluate and benchmark ONTRAMs in terms of prediction performance and interpretability. For the experiments we use two publicly available datasets as presented in the following section. In addition, we simulate tabular predictors to assess estimation performance of ONTRAMs.

4.1 Data

Wine quality: The Wine quality dataset consists of 4898 observations [Cortez et al., 2009]. The ordinal outcome describes the wine quality measured on a scale with 10 levels of which only 6 consecutive classes (3 to 8, $n_3 = 10$, $n_4 = 53$, $n_5 = 681$, $n_6 = 638$, $n_7 = 199$, $n_8 = 18$) are observed. The dataset contains 11 predictors, such as acidity, citric acid and sugar content. As in Gal and Ghahramani [2016], we consider a subset of the data (red wine, $n = 1599$).

UTKFace: UTKFace contains more than 23000 images of peoples' faces of all age groups. The images are labeled with the people's age (0 to 116), gender (female, male) and ethnicity (Asian, Black, Indian, White, Others). As an ordinal outcome we considered the variable age group with classes baby (0–3, $n_0 = 1894$), child (4–12, $n_1 = 1519$), teenager (13–19, $n_2 = 1180$), young adult (20–30, $n_3 = 8068$), adult (31–45, $n_4 = 5433$), middle aged (46–61, $n_5 = 3216$) and senior (>61, $n_6 = 2395$). As our main goal is not on performance improvement but on the evaluation of our proposed methods, we use the already aligned and cropped versions of the images. For some example images see Appendix F.

<https://hal.inria.fr/hal-01892103/document>
Available at <https://susanqq.github.io/UTKFace/>

Simulated tabular predictors: We simulate tabular predictors \mathbf{x} with predefined effects on the ordinal outcome of the UTKFace dataset, where we assume a proportional odds model $F_Y(y_k|\mathbf{x}) = F_Z(\vartheta_k - \mathbf{x}^\top \boldsymbol{\beta})$ (see Section 2.2.2). The simulation scheme is closely related to choice-based sampling [Manski and Lerman, 1977]. Ten predictors are simulated, four of which are noise predictors that have no effect on the outcome. The six informative predictors are simulated to have an effect of $\pm \log 1.5$, $\pm \log 2$ and $\pm \log 3$ on the log-odds scale, to reflect small to large effect sizes commonly seen in medical and epidemiological applications [Cohen, 1992]. All predictors are mutually independent of each other and the image data. The predictors are simulated from the conditional distribution $X_j|\mathbf{y} \sim \mathcal{N}(\mathbf{y}^\top \boldsymbol{\xi}_j, \sigma^2)$, where \mathbf{y} denotes the one-hot encoded outcome and $(\boldsymbol{\xi}_j)_k = k \cdot \beta_j$ for $k = 1, \dots, K$, to emulate the proportional odds property. All simulated predictors have a common variance of $\sigma^2 = 1.55^2$, which was tuned such that the estimated $\hat{\beta}_j$ on average recovers the true β_j when estimating the conditional distribution $Y|\mathbf{x}$ in a proportional odds model. A summary of the simulation procedure is given in Figure 5.

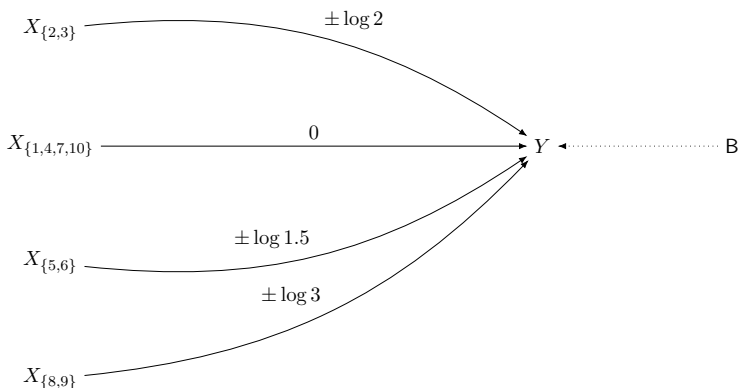


Figure 5: Simulation of predictors for UTKFace data. $X_j \stackrel{\text{i.i.d.}}{\sim} \mathcal{N}(0, \sigma^2)$, $j = 1, \dots, 10$, with $\sigma^2 = 1.55^2$. The predictors X_j are simulated such that their effects adhere to the proportional odds assumption. That is, the effect of $\boldsymbol{\beta}$ is common to all class boundaries. Note that the arrows indicate effects on the log-odds scale of the outcome Y , i.e., $F_Y(y_k|\mathbf{x}) = F_L(\vartheta_k - \mathbf{x}^\top \boldsymbol{\beta})$. The dotted arrow from \mathbf{B} to Y indicates that the image is not entering the simulation directly but is assumed to have an effect on the outcome.

4.2 Models

The models we use for evaluating and benchmarking the proposed ONTRAMs are summarized in Table 1. These models feature a different flexibility and interpretability and are trained with the different loss functions described in Sections 2 and 3. In Section 4.3 we introduce the evaluation procedures and applications of these models. Section 4.4 summarizes the NN architectures for the ONTRAMs. In Section 5 we present and discuss the results of these models.

4.3 Experimental Setup

Wine quality: The wine quality dataset contains purely tabular predictors. We use this dataset to benchmark the proportional odds ONTRAM (SI-LS $_{\mathbf{x}}$) against a proportional odds model fit (`tram:polr`) within the statistical computing environment R and compare both models in terms of prediction performance and estimated effects. As a more complex model we fit a GAM in the ONTRAM framework and compare it to an implementation of GAMs for proportional odds

Table 1: Summary of the models used for evaluating the ONTRAM methods. In the upper part we list models used for the Wine data which contain only tabular predictors (\mathbf{x}), below models for the UTKFace data which consist of image data and tabular predictors (\mathbf{x}, \mathbf{B}). Above the thin lines we list the baseline models; below the ONTRAMs. For each model which can be framed as a transformation model the transformation function is given. Parameters in the shift terms of a transformation function can be interpreted as log odds-ratios if F_Z is chosen to be the standard-logistic distribution.

Dataset	Model name	Abbreviation	Trafo $h(y_k D)$
Wine	Multi-class classification	MCC	
	Generalized additive proportional odds model	GAM	$\vartheta_k - \sum_{j=1}^p \beta_j(x_j)$
	Proportional odds logistic regression	polr	$\vartheta_k - \mathbf{x}^\top \boldsymbol{\beta}$
	Complex intercept	$\text{CI}_{\mathbf{x}}$	$\vartheta_k(\mathbf{x})$
	Simple intercept + GAM complex shift	$\text{SI-CS}_{\mathbf{x}}^*$	$\vartheta_k - \sum_{j=1}^p \beta_j(x_j)$
	Simple intercept + linear shift	$\text{SI-LS}_{\mathbf{x}}$	$\vartheta_k - \mathbf{x}^\top \boldsymbol{\beta}$
UTKFace	Multi-class classification	MCC	
	Multi-class classification + tabular	$\text{MCC-}\mathbf{x}$	
	Complex intercept	$\text{CI}_{\mathbf{B}}$	$\vartheta_k(\mathbf{B})$
	Complex intercept + tabular	$\text{CI}_{\mathbf{B}}\text{-LS}_{\mathbf{x}}$	$\vartheta_k(\mathbf{B}) - \mathbf{x}^\top \boldsymbol{\beta}$
	Simple intercept + complex shift	$\text{SI-CS}_{\mathbf{B}}$	$\vartheta_k - \eta(\mathbf{B})$
	Simple intercept + complex shift + tabular	$\text{SI-CS}_{\mathbf{B}}\text{-LS}_{\mathbf{x}}$	$\vartheta_k - \eta(\mathbf{B}) - \mathbf{x}^\top \boldsymbol{\beta}$
	Simple intercept + tabular	$\text{SI-LS}_{\mathbf{x}}$	$\vartheta_k - \mathbf{x}^\top \boldsymbol{\beta}$

logistic regression in R (`mgcv::gam`). Furthermore, we use the data to investigate how the training performance changes for different sample sizes when applying the different loss parametrizations in the $\text{CI}_{\mathbf{x}}$ ONTRAM and the MCC model.

For analyses of the wine quality data we employ the same cross-validation scheme as Gal and Ghahramani [2016] and split the data into 20 folds of 90% training and 10% test data. The predictors are normalized to the unit interval. Otherwise, no further preprocessing is performed. All models are trained via stochastic gradient descent using a learning rate of 0.001. The linear shift model is trained for 8000 epochs with a batch size of 90. The ONTRAM GAM is trained for 1200 epochs with a batch size of 180. All other models for the wine data in Table 1 are trained for 100 epochs with a batch size of 6.

UTKFace: The UTKFace dataset consists of image data and contains information on an individual’s sex, which will be used to explore the interpretability of different ONTRAMs. In addition, we add simulated tabular predictors, which allows us to fit a cascade of models incorporating image and/or tabular data in different ways (see Table 1). By fitting simple shift ($\text{-LS}_{\mathbf{x}}$) models, we investigate if the estimated log odds-ratios $\hat{\boldsymbol{\beta}}$ can recover the known, true effects $\boldsymbol{\beta}$ from the simulation. For that we consider several models with ($\text{CI}_{\mathbf{B}}\text{-LS}_{\mathbf{x}}$, $\text{SI-CS}_{\mathbf{B}}\text{-LS}_{\mathbf{x}}$) or without ($\text{SI-LS}_{\mathbf{x}}$) image data. Moreover, we assess prediction performance and interpretability when adding different input data and model components and discuss the most appropriate ONTRAM for the task at hand. To have a fair baseline comparison to the ONTRAMs, we consider the two models MCC and $\text{MCC-}\mathbf{x}$ including image as well as image and simulated tabular data.

The UTKFace dataset is split into a training (80%) and a test set (20%); 20% of the training set is used as validation data. The images are resized to $128 \times 128 \times 3$ pixels. The resized images

are normalized to have pixel values between 0 and 1. No further preprocessing is performed. The models are trained for up to 100 epochs with the Adam optimizer with a batch size of 32 and a learning rate of 0.001. Overfitting is addressed with early stopping. That is, we retrospectively search for the epoch in which the validation loss is minimal and consider the respective parameters for our trained models.

We analyse the dataset using deep ensembling [Lakshminarayanan et al., 2017]. Specifically, models are trained five times with a different weight initialization in each iteration. The resulting predicted conditional outcome distribution is averaged over the five runs and this averaged conditional outcome distribution is then used for model evaluation. This procedure is supposed to prevent double descent [Oppen et al., 1990] and improve test performance [Belkin et al., 2019, Wilson and Izmailov, 2020].

Wine, UTKFace: We use both datasets to highlight the advantages of using a proper (MCC and ONTRAM) over an improper scoring rule as loss functions in ordinal regression. In Appendix E, we contrast ordinal regression and classification.

4.4 Neural network architectures

We use NNs with different architectures to explore the various additive decompositions of the transformation function described in Section 3. Simple intercept and linear shift terms are always modeled with single layer NNs without bias terms and a linear activation function (see left panel in Figure 4). For a fair comparison, we use the same NN architecture for all MCC models and for controlling the complex intercept or complex shift term in an ONTRAM. The only difference between the models is in the output layer. MCC models feature an output layer with K units and a softmax activation function. The output layer of complex intercept terms has $K - 1$ output units and a linear activation function. In case of complex shift terms, the output layer consists of one unit and a linear activation function.

Wine quality: MCC models, CI and CS terms are modeled using a densely connected neural network with four layers having 16 units each. Between layers 1, 2, and 3, we specify a dropout layer with dropout rate 0.3 [Srivastava et al., 2014]. ReLU is used as the activation function. GAMs are fitted using the same densely connected neural network for each predictor with two layers of 16 units and followed by a layer of eight units with ReLU activation. All weights were regularized using both L_1 and L_2 penalties, with $\lambda_1 = 1$ and $\lambda_2 = 5$. Between each layer there is dropout with rate 0.2.

UTKFace: MCC, CI and CS terms are modeled with a CNN (see Figure 6). The architecture used in this work is inspired by the VGG [Simonyan and Zisserman, 2014]. The convolutional part consists of three blocks while each block is comprised of two convolution and two dropout layers (with dropout rate 0.3). The blocks complete with a max-pooling layer (window size 2×2 pixels, stride width 2). In the first block we use 16 filters; the following two blocks contain 32. Filter size is fixed to 3×3 pixels in every block. The fully connected part features a 500- and a 50-unit fully connected layer. The ReLU non-linearity is used as the activation function.

4.5 Software

We implement MCC models and ONTRAMs in the two programming languages R 3.6 and Python 3.7 [R Core Team, 2020, Van Rossum and Drake Jr, 1995]. The models are written in `Keras` based on a `TensorFlow` backend using `TensorFlow` version >2.0 [Chollet et al., 2015, Abadi et al., 2015] and trained on a GPU. Both `polr` and generalized additive proportional odds models are fitted in R using

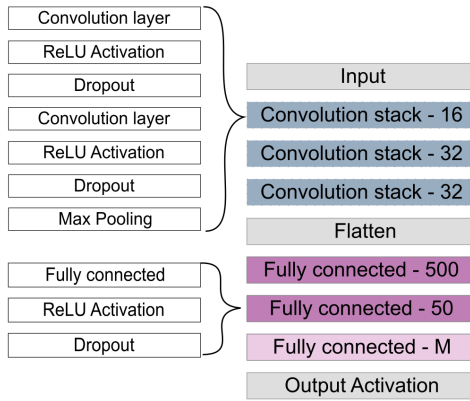


Figure 6: CNN architectures for controlling MCC models, complex intercept and complex shift terms in case of image input data. The network architecture consists of stacks of convolutional blocks consisting of multiple repetitions of a convolutional, dropout and batch-normalization layer, followed by a fully connected part.

`tram::polr()` [Hothorn, 2020b] and `mgcv::gam()` [Wood, 2017], respectively. Further analysis and visualization is performed in R. For reproducibility, all code is made available on GitHub.

4.6 Model evaluation

Evaluation metrics: We evaluate the prediction performance of all ONTRAMs with proper scoring rules, namely the negative log-likelihood (NLL) and the ranked probability score (RPS). Roughly speaking, proper scoring rules encourage honest probabilistic predictions because they take their optimal value when the predicted conditional outcome distribution corresponds to the data generating distribution (for details see Appendix D).

Estimation and interpretability: To evaluate estimation performance, in proportional odds ONTRAMs containing a linear shift term in \mathbf{x} ($LS_{\mathbf{x}}$), we make use of the simulated tabular predictors and compare the known true effects of the individual predictors to the estimates. This ensures the correct interpretation of the predictors' effects.

5 Results and discussion

The results for the MCC models and ONTRAMs are given in the following Sections 5.1 and 5.2.

5.1 Wine quality

The wine dataset with its ordinal outcome and tabular predictors represents a typical use case for a proportional odds model, which allows to interpret the fitted effects as log odds-ratios (see Section 2.2.2). In the ONTRAM framework we fit a proportional odds model via a $SI-LS_{\mathbf{x}}$ model. We fit the same model using `tram::Polr()`. As expected, Figure 7 shows that both models yield the same prediction performance in terms of NLL (A) and RPS (B) and estimated predictor effects (C).

<https://www.github.com/LucasKookUZH/ontram-paper>

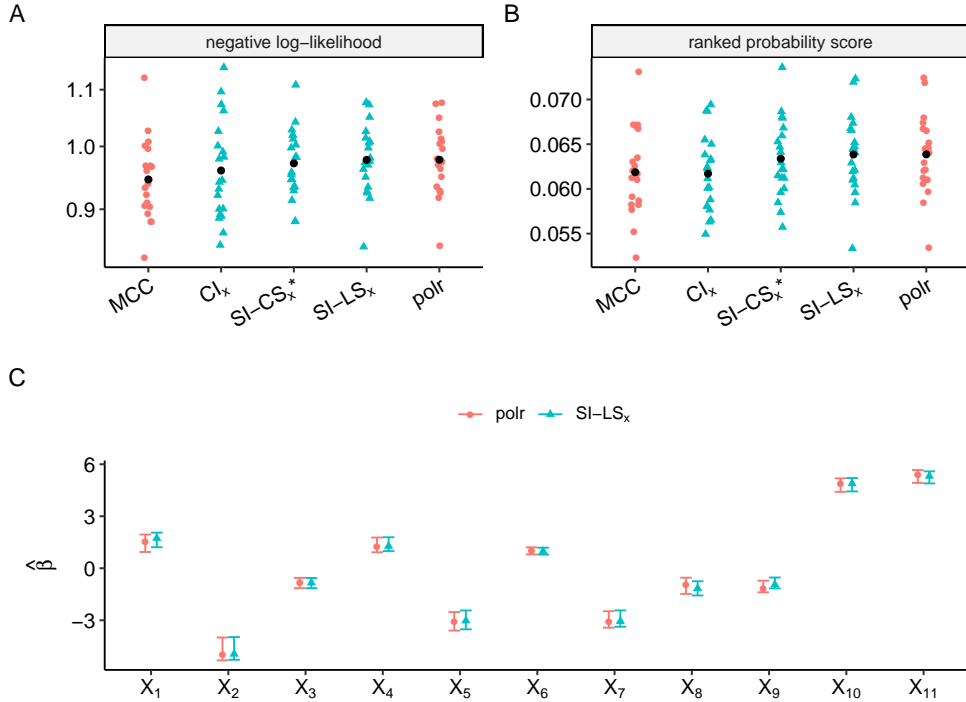


Figure 7: Results of the wine quality data based on the test sets from the cross validation setting. Panels A and B summarize the prediction performance for the models MCC, CI_x , GAM, $SI-LS_x$ and polr (x-axes) based on the wine quality dataset in terms of negative log likelihood (A) and ranked probability score (B). Lower values in NLL and RPS indicate improved model performance. Results of ONTRAMs are indicated as blue triangles, others as red dots. The black point gives the mean across the respective metric resulting from the single CV folds. C: Effect estimates with 2.5th and 97.5th percentile for polr and $SI-LS_x$ model over the 20 CV folds of the wine quality dataset.

GAMs add another layer of complexity to the model by allowing non-linear effects for each predictor. Because the individual NNs do not interact explicitly the estimated log odds-ratio function retains the interpretability of a proportional odds model. Figure 8 depicts the estimates of an ensemble of ONTRAM GAMs in comparison to a GAM from the R-package **mgcv**. Apart from the constraint-enforced smoothness in **mgcv**'s GAM, both models agree in magnitude and shape of the estimated predictor effects. For instance, predictor X_{10} (sulphate content) has a strong positive influence on the rating when increased from 0 to 0.25 (on the transformed scale), in that the odds of the wine being rated higher increase by a factor of 7.4, all other predictors held constant ($\exp(\hat{\beta}_{10}(0.25) - \hat{\beta}_{10}(0)) \approx \exp(2) \approx 7.4$). Afterwards the effect levels off and stays constant for the ONTRAM GAM, due to regularization and few wines with higher sulphate levels being present in the training data. The curve estimated by **mgcv** follows smoothness constraints and instead drops with a large confidence interval, also covering 0. GAMs are a special case of complex shift models, the latter of which allow for higher order interactions between the predictors. Conceptually, ONTRAMs allow to further trade off interpretability and flexibility by modelling some predictor effects linearly while including others in a complex shift or intercept term. If field knowledge suggests non-linearity of effects or interacting predictors they can be included as a complex shift or, if the proportionality assumption is violated, in a complex intercept. From Figure 8 we can see that

most of the coefficients could be safely modelled in a linear fashion, which is also evident from the minor loss in predictive power when comparing the GAM against the linear shift ONTRAM (see Figure 7 A, GAM *vs.* SI-LS $_{\mathbf{x}}$).

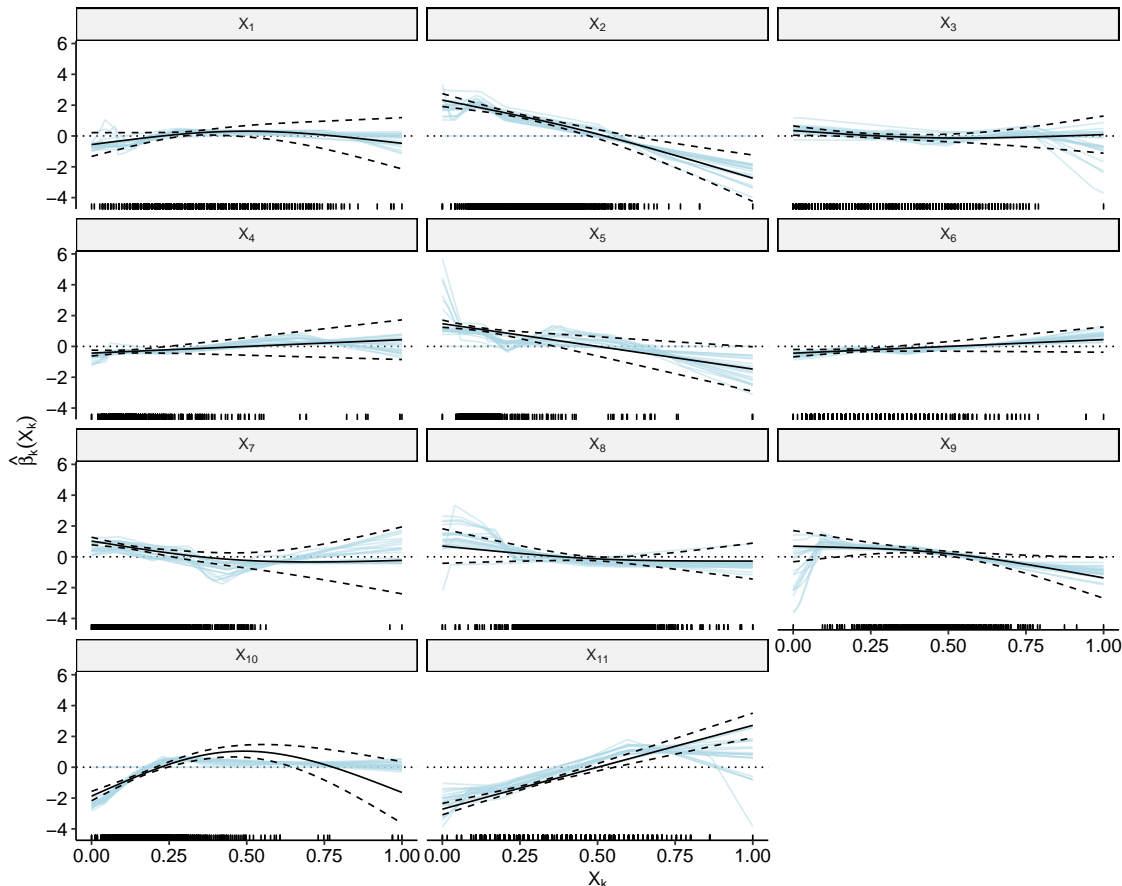


Figure 8: Estimated log odds-ratio functions in the ONTRAM GAM model for the wine quality data. The estimates of an ensemble of 20 runs with different initial weights are shown in blue for each of the eleven predictors. The solid black line depicts the estimated log odds-ratio functions estimated by the `mgcv::gam()` function in R together with a 95% confidence interval (dashed black lines). Rugs on the bottom of each plot indicate the observed values for X_k , $k = 1, \dots, 11$, in the training data.

The most flexible $\text{CI}_{\mathbf{x}}$ ONTRAM and the MCC model, which solely differ in the parametrization of their NLL loss, show the expected agreement in achieved prediction performance w.r.t. NLL and RPS (see Figure 7 A and B). However, the $\text{CI}_{\mathbf{x}}$ model learns much faster in terms of number of epochs until the minimum test loss is reached, compared to the MCC model. We attribute this to the parametrization of the ONTRAM loss, because unlike the categorical cross-entropy, it takes the ordering of the outcome into account. To further investigate this gain in learning speed, we split the wine quality data into n/n_t , $n_t \in \{50, 100, 200, 480\}$ folds of size n_t and fit a MCC model and $\text{CI}_{\mathbf{x}}$ ONTRAM to each fold. The median test loss is computed for each scenario of size n_t . The number of epochs needed to achieve minimal median test loss is summarized in Figure 9 A. The training speed is consistently lower and therefore more efficient for the $\text{CI}_{\mathbf{x}}$ ONTRAM than for the MCC model (Figure 9 A). The $\text{CI}_{\mathbf{x}}$ ONTRAM yields a slightly better prediction performance (median

test NLL) for larger sample sizes, because after 200 epochs the MCC model still has not reached the minimum test loss (Figure 9 B). Note that the performance gain is only present if the outcome is truly ordered. In Appendix A, we show that the effect vanishes when the ordered class labels are permuted.

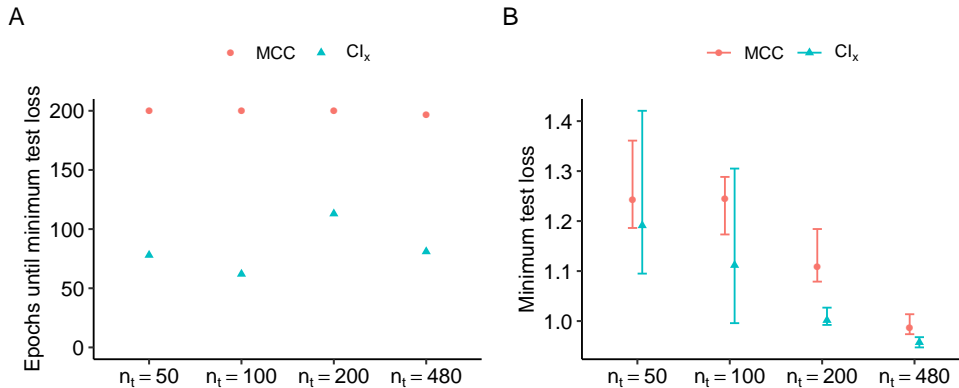


Figure 9: Epochs until minimum test loss for varying sizes of the training data using the wine quality dataset. The data are split into n/n_t , $n_t \in \{50, 100, 200, 480\}$ folds each of which serves as training data for a multi-class classification and a complex intercept ONTRAM. The median test loss is computed for each scenario n_t and each epoch. Afterwards, the number of epochs until minimum median test loss and the minimum median test loss are recorded. Here the epochs until minimum test loss (A) and the minimum test loss (B) are plotted against the 4 scenarios given by n_t .

5.2 UTKFace

Seven models are fitted to the UTKFace dataset with the simulated tabular predictors (see Table 1). Those models differ in the usage of tabular predictors or image data as input, the flexibility of the transformation and the loss function. Here, we consider proper scoring rules (NLL & RPS) to evaluate the seven regression models, which aim to predict a valid conditional outcome distribution by using a NLL loss (MCC models and ONTRAMs). In Appendix E, we compare the MCC model and the CI_x ONTRAM to the ordinal classification model trained with a loss based on the quadratically weighted Cohen’s kappa [de La Torre et al., 2018] in terms of classification performance (QWK).

First, we evaluate the most flexible models, MCC and CI_B with image data as input. As expected, both models yield comparable prediction performances in terms of NLL and RPS (see Figure 10 A and B). Adding simulated tabular predictors increases the performance in both models notably (see MCC- x and CI_B -LS $_x$ in Figure 10 A and B). In the case of the MCC- x model, the tabular predictors are attached to the feature vector resulting from the convolutional part of the CNN allowing for interactions between the inputs. Including image data as a complex shift rather than a complex intercept yields a less flexible but more interpretable model (SI-CS $_B$). Although the complex shift model is less flexible than the complex intercept model, prediction performance is comparable to the CI_B ONTRAM. Adding simulated tabular data as a linear shift term (SI-CS $_B$ -LS $_x$) again results in a large improvement. Using only the simulated tabular data for age estimation (SI-LS $_x$) yields a better performance than the models that solely include image data (MCC, CI_B , SI-CS $_B$). However, adding image data to the tabular predictors further improves

prediction performance (SI-LS $_x$ vs. MCC- x and CI $_B$ -LS $_x$ and SI-CS $_B$ -LS $_{rx}$). This indicates that

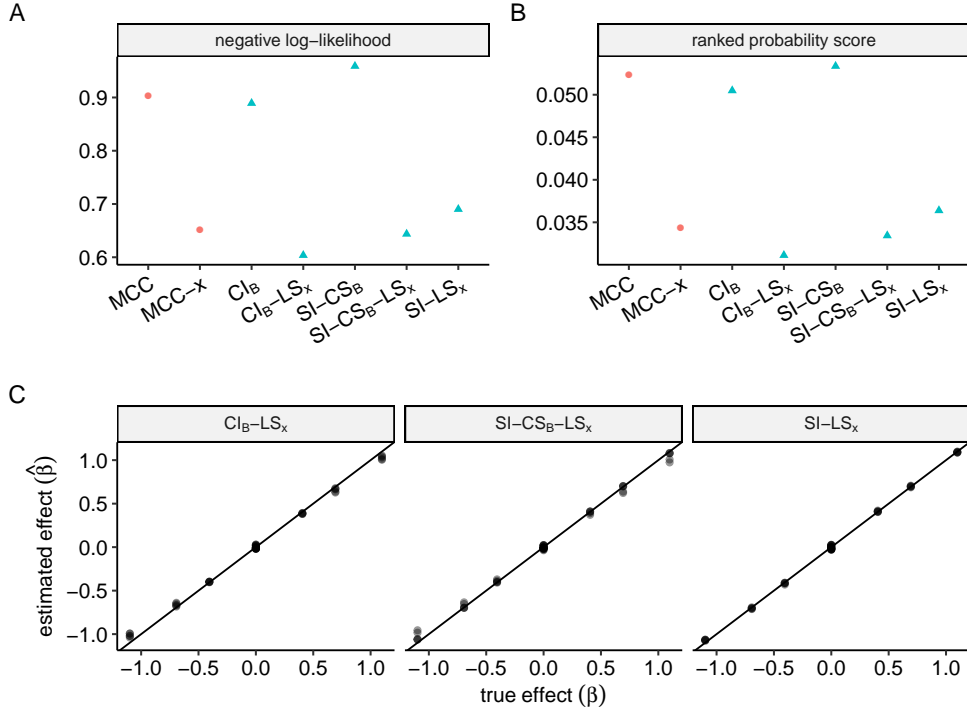


Figure 10: Test prediction performance for deep ensembles based on the UTKFace data. The figure summarizes the results for the models MCC, MCC- x , CI $_B$, CI $_B$ -LS $_x$, SI-CS $_B$, SI-CI $_B$ -LS $_x$, SI-LS $_x$ (x-axes) in terms of negative log-likelihood (A) and ranked probability score (B). Lower values in NLL and RPS indicate improved model performance. Baseline models are highlighted in red, ONTRAMs in blue. C: True versus estimated predictor effects. The figure summarizes the true versus estimated effects of the simulated tabular predictors of the UTKFace dataset. The effect estimates result from the linear shift terms, LS $_x$, in the models CI $_B$ -LS $_x$, SI-CS $_B$ -LS $_x$, SI-LS $_x$. In case of correct estimation, the parameters lie on the main diagonal.

the images contain useful information for the prediction task. In practice, the ONTRAMs CI $_B$ -LS $_x$ and SI-CS $_B$ -LS $_x$ are most attractive because they provide interpretable estimates for the effects of the tabular predictors with an acceptably low decrease in prediction performance.

As discussed before, the effect estimates resulting from the linear shift terms $\mathbf{x}^\top \boldsymbol{\beta}$ of ONTRAMs (CI $_B$ -LS $_x$, SI-CS $_B$ -LS $_x$, SI-LS $_x$) can be interpreted as log odds-ratios. Because the data are simulated, we know the true effect β for each predictor and estimate the effect $\hat{\beta}$ from the data. As summarized in Figure 10 C, all models can recover the correct estimates.

Lastly, we feature the case of interpreting a predictor, which to a certain extent is contained within the image. In this case we investigate the effect of a person’s sex on the predicted age category, which is more or less clearly contained in the image; think of, e.g., babies. In the model that solely includes sex as a predictor (SI-LS $_{\text{sex}}$), the estimated coefficient is easily interpreted as a decrease in the odds of belonging to a higher category by a factor of $\exp(-0.5) = 0.6$, when comparing female to male (see Figure 11 B), because there are more younger women in the dataset (see Table F1). When including the image in the model the prediction performance improves and due to co-linearity of sex and image the estimated effect $\hat{\beta}_{\text{sex}}$ not only shrinks towards zero, but flips

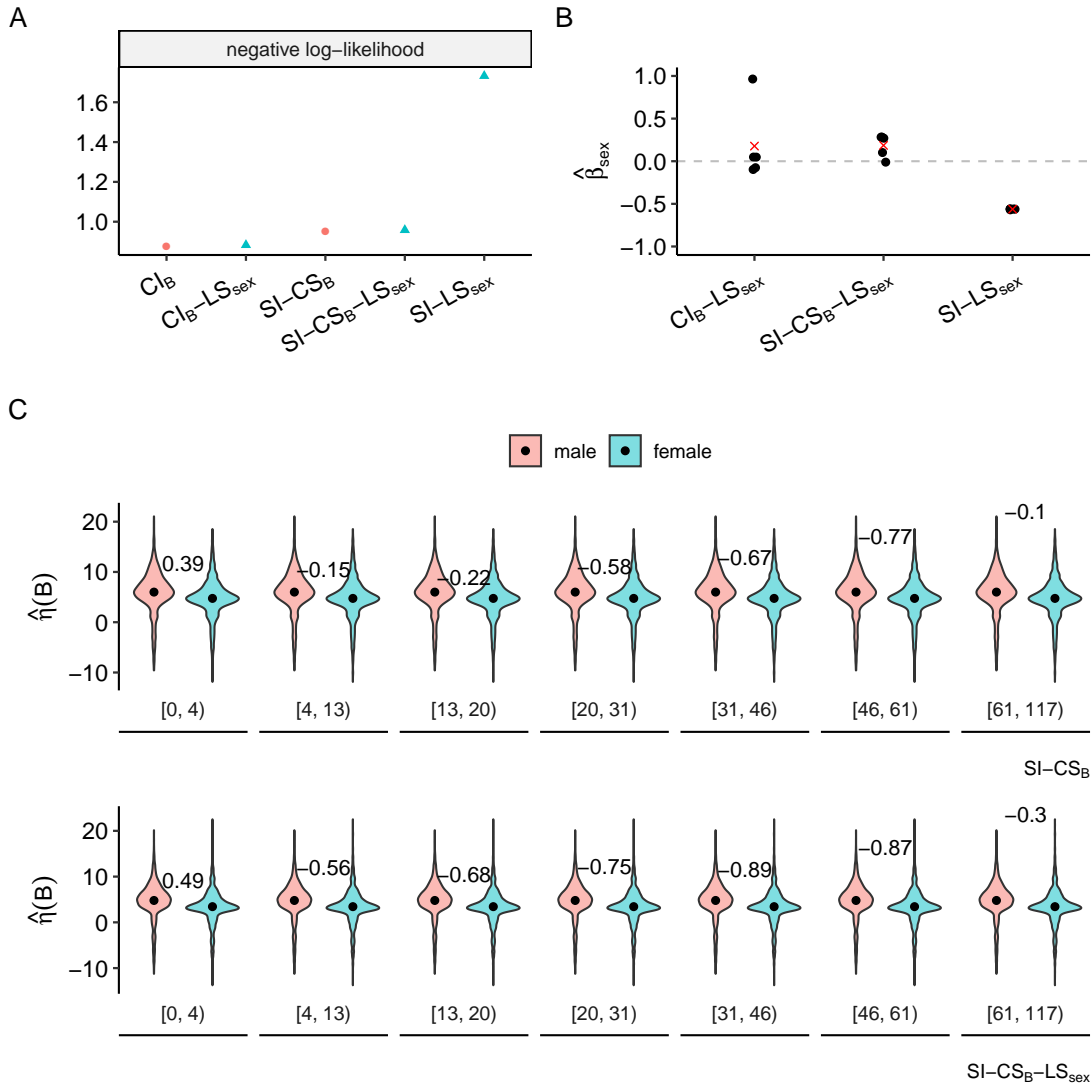


Figure 11: Interpretability of estimates for β_{sex} in the UTKFace data. A: Test prediction performance in terms of NLL is given for the model that includes solely sex and the complex shift and intercept models with and without sex included in a linear shift term. Each test prediction is derived from an ensemble of five individual models. B: Effect estimates for each model included in the ensemble. The estimated coefficients for sex differ for the model which does not include the image compared to the complex intercept and shift models, because the effect of sex is adjusted for the image. C: Estimated log odds-ratios $\hat{\eta}(B)$ for the complex shift model, with (upper) and without (lower) including sex as a predictor, stratified by age group and sex.

its sign (Figure 11 A). It is now much harder to interpret the effect of sex directly, while “holding an image constant”. To do so, it is helpful to visualize the estimated image log odds-ratios, $\hat{\eta}(B)$ stratified by age group and sex for both a model that includes sex and does not include sex as a predictor (Figure 11 C). Images depicting a women are associated with a lower estimated log odds-ratio on average for age groups 1–6 in both models. When sex is explicitly adjusted for in the model, the mean difference in log odds-ratios between female and male get larger ($SI\text{-CS}_B\text{-LS}_{\text{sex}}$).

In turn, these estimate has to be interpreted together with the estimate $\hat{\beta}_{\text{sex}}$, by adding it to the estimated image log odds-ratios for females. Including the image allows a more direct interpretation than in the linear shift model, in that, on average, women are estimated to be younger than men for age groups other than babies in this observational dataset.

6 Conclusion and outlook

In this work we demonstrate how to unite the classical statistical approach to ordinal regression with deep learning models while preserving interpretability of selected model components. We show that the effects of the tabular predictors are correctly estimated, also in the presence of complex image data. In addition, the cumulative ordinal parametrization of the NLL leads to more efficient learning compared to the standard parametrization of the categorical cross entropy for ordered outcomes.

We demonstrate how to choose the most appropriate model in a top-down modeling strategy and end up with a model that possesses the most useful degree of interpretability while still showing an adequate prediction power. Interpretability of the different model components was showcased for simple models including only tabular predictors and more complex models in which tabular predictors may be highly co-linear to some of the information encoded in the image. The modular nature of our ONTRAMs makes them highly versatile and applicable to many other problems with ordinal outcome and complex input, such as text or speech data.

This work shows the potential of deep transformation models for ordinal outcomes. The predictive power of deep transformation models on regression problems with continuous outcomes has already been demonstrated [Sick et al., 2020]. However, the approach is easily extendable to the full range of existing interpretable regression models, including models for count and survival outcomes. The extension from ordinal data to count and survival data is hinted at by the parametrization of the ONTRAM NLL, which can be viewed as an interval-censored log-likelihood over the latent variable Z for which the intervals are given by the conditional cut points $h(y_k|D)$. For count data these cut points are given by consecutive integers, i.e., $(0, 1]$, $(1, 2]$, etc.. In survival data the interval is given by (commonly) right censored outcomes when a patient drops out of a study or dies due to a competing risk. In case of right-censoring the interval is given by $(t, +\infty)$ for a patient that drops out at time t . All benefits in terms of interpretability and modularity will carry over to the deep conditional transformation version of other probabilistic regression models by working with an appropriate likelihood and parametrizing the transformation function via (deep) neural networks.

Acknowledgements

We would like to thank Elvis Murina and Muriel Buri for insightful discussions. Interpretation of the effects of image and sex on the predicted age category is done in terms of averages and thus is without prejudice towards individuals in terms of sex, gender or ethnicity and limited specifically to the observational UTKFace dataset.

A Learning speed under permuted class labels

In contrast to MCC models with categorical cross-entropy loss, ONTRAMs’ loss parametrization take the ordering of the outcome into account (see equation 3). This leads to more efficient learning when the outcome is truly ordered. This can be demonstrated by permuting the class label ordering of a truly ordinal outcome and inspecting the learning curves of an ONTRAM and MCC model. When fitting the model using the true class label ordering, the ONTRAM outperforms the MCC model in terms of learning speed and arrives at virtually the same minimum test loss (*cf.* Figure A1). Permuting the class label order does not affect the learning curves of the MCC model. However, the complex intercept ONTRAM performs on-par in the presence of wrongly ordered categories in learning speed and median test loss compared to the MCC model. In general, we observe a higher variability in the loss curves between different runs when using the ONTRAM loss parametrization.

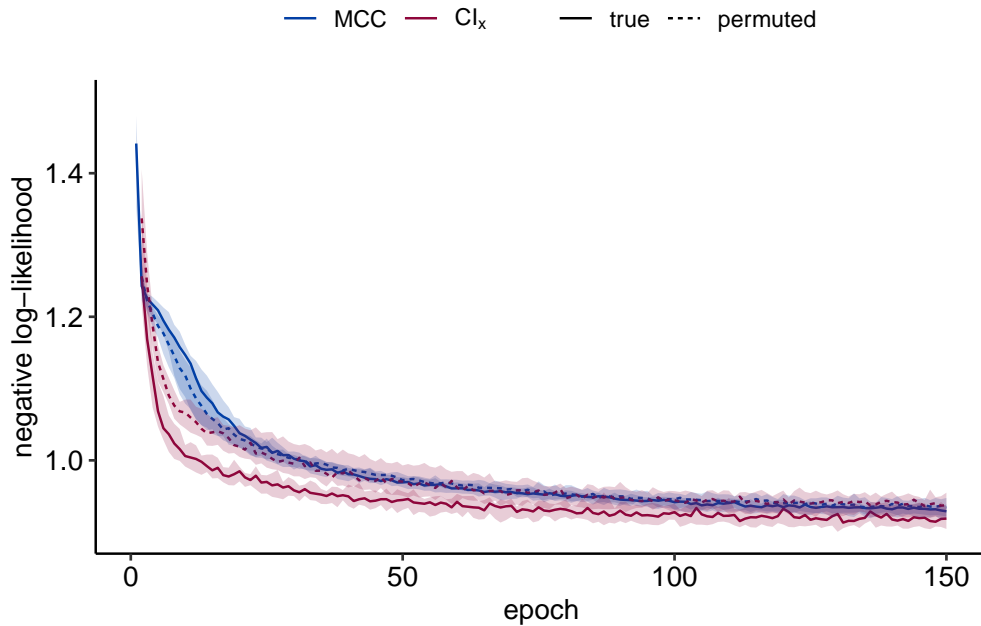


Figure A1: Test learning curves comparing a MCC against a complex intercept model (CI_x) for the true and a permuted ordering of the classes in the wine quality dataset. Depicted are the median test losses (thick line) together with the empirical 20th and 80th percentile (shaded regions) over 20 runs.

B Interpretational scales

Classical regression textbooks, like Tutz [2011], discuss $F_Z \in \{F_L, F_{MEV}, F_{Gumbel}, \Phi\}$, which are called cumulative logit, minimum extreme value, maximum extreme value and probit models, respectively. Tutz [2011] also derives the interpretational scales and stresses, that the parameters resulting from a cumulative probit model are hard to interpret.

Table B1: Interpretational scales induced by F_Z [Tutz, 2011].

F_Z	F_Z^{-1}	Symbol	Interpretation of β and η
Logistic	logit	$F_L = \text{expit}$	log odds-ratio
Gompertz	cloglog	F_{MEV}	log hazard-ratio
Gumbel	loglog	F_{Gumbel}	log hazard-ratio for $Y_r = K + 1 - Y$
Normal	probit	Φ	not interpretable directly

For $F_Z = F_L := (1 + \exp(-z))^{-1}$ in a linear shift model $h(Y = y_k | x) = \vartheta_k - \mathbf{x}^\top \beta$

$$\begin{aligned}
 \mathbb{P}(Y \leq y_k | \mathbf{x}) &= F_L(\vartheta_k - \mathbf{x}^\top \beta) \\
 \Leftrightarrow \text{logit}(\mathbb{P}(Y \leq y_k | \mathbf{x})) &= \vartheta_k - \mathbf{x}^\top \beta \\
 \Leftrightarrow \log(\text{odds}(Y \leq y_k | \mathbf{x})) &= \vartheta_k - \mathbf{x}^\top \beta \\
 \Leftrightarrow \log(\text{odds}(Y \leq y_k | \mathbf{x})) &= \log(\text{odds}(Y \leq y_k | \mathbf{x} = 0)) - \mathbf{x}^\top \beta \\
 \Leftrightarrow -\log(\text{odds}(Y > y_k | \mathbf{x})) &= -\log(\text{odds}(Y > y_k | \mathbf{x} = 0)) - \mathbf{x}^\top \beta \\
 \Leftrightarrow \text{odds}(Y > y_k | \mathbf{x}) &= \text{odds}(Y > y_k | \mathbf{x} = 0) \cdot \exp(\mathbf{x}^\top \beta),
 \end{aligned}$$

which shows that the components of β are interpretable as log odds-ratios. In the same way, $\eta(\mathbf{B})$ in a complex shift model can be interpreted as a log odds-ratio function. Table B1 summarizes the four most commonly used cumulative ordinal regression models and the interpretational scales that different F_Z induce.

For $F_Z = F_{\text{MEV}} = 1 - \exp(-\exp(z))$ we can interpret the components of β as log hazard ratios

$$\begin{aligned}
 1 - F_Y(y | \mathbf{x}) &= \exp(-\exp(h(y) + \mathbf{x}^\top \beta)) = \exp(-\exp(h(y)) \exp(\mathbf{x}^\top \beta)) \\
 &= \exp(-\exp(h(y)))^{\exp(\mathbf{x}^\top \beta)} = (1 - F_Y(y | \mathbf{x} = 0))^{\exp(\mathbf{x}^\top \beta)}.
 \end{aligned}$$

This interpretational scale is commonly used in survival analysis [Collett, 2015]. Here, a log hazard ratio β for a shift from 0 to \mathbf{x} is defined in terms of the conditional survivor function $S_Y(y | \mathbf{x}) = 1 - F_Y(y | \mathbf{x})$ given by $S_Y(y | \mathbf{x}) = S_Y(y | \mathbf{x} = 0)^{\exp(\mathbf{x}^\top \beta)}$.

C Ordinal classification with Cohen’s kappa

Recently, DL models for ordinal classification were introduced using a transformed continuous version of the quadratic weighted kappa (QWK) as the loss function [de La Torre et al., 2018]. Cohen’s kappa is usually used to assesses inter-rater agreement and corrects it for the expected number of agreements under independence [Cohen, 1960]

$$\kappa = \frac{p_{\text{obs}} - p_{\text{exp}}}{1 - p_{\text{exp}}}, \tag{19}$$

where p_{obs} and p_{exp} are the observed and expected proportion of agreement under independence. They are computed from a confusion matrix, after dividing all entries by the number of predicted instances, p_{obs} is given by the sum of the diagonal elements and p_{exp} by the diagonal sum of the product of the row and column marginals. An additional weighting scheme enables to penalize misclassifications far away from the observed class more strictly [Cohen, 1968] than misclassifications

close to the observed class

$$\kappa_w = \frac{\sum_{i,j} w_{ij} o_{ij} - \sum_{i,j} w_{ij} e_{ij}}{1 - \sum_{i,j} w_{ij} e_{ij}}, \quad (20)$$

where e denotes the expected and o the observed number of agreements in row i and column j of a confusion matrix. The weights $w_{ij} = \frac{|i-j|^q}{(K-1)^p}$ and the exponent q control the amount of penalization for predictions farther away from the observed class. Because Cohen’s kappa considers the ordinal nature of the outcome when weighted accordingly, it has been proposed and used as a loss function for deep ordinal classification problems [de La Torre et al., 2018, 2020, Vargas et al., 2019, 2020]. The QWK loss is defined as

$$\ell(p) = \log(1 - \kappa(p)), \quad (21)$$

where p is the predicted probability distribution and denotes the quadratically ($q = 2$) weighted Cohen’s kappa. Originally defined for count data, de La Torre et al. [2018] generalized Cohen’s kappa to be computable from a probability density and so be used as a loss function for MCC networks (when using softmax in the last layer). However, the QWK loss is an improper scoring rule and thus does not yield calibrated probabilistic predictions (cf. Appendix D). As such, we demonstrate its limited use in estimating conditional distributions for ordinal outcomes in Appendix E. However, if one were solely interested in ordinal classification, the QWK loss is useful to penalize misclassifications farther away from the observed class, where the weighting scheme controls the amount of penalization. Ordinal regression and classification are contrasted in more detail in Appendix E.

To contrast ordinal regression models with pure classification models we additionally use evaluation metrics for ordinal classifiers, such as the accuracy, continuous QWK (the QWK loss transformed back to its original scale via $1 - \exp(\ell(p))$, see eq. (21)), and discrete QWK (see eq. (20)). Neither accuracy nor the QWK metrics are proper scoring rules and both can lead to misleading results when evaluating probabilistic models (cf. Appendix E and D).

D Scoring rules

Here we give a brief overview on scoring probabilistic predictions. In the end we show that the QWK loss is an improper scoring rule.

Scoring rules are used to judge the prediction quality of a probabilistic model and have their roots in information theory and weather forecasting [Gneiting and Raftery, 2005]. On average, a strictly proper scoring rule only takes its optimal value if the predicted probability distribution corresponds to the “data generating” probability distribution. Assume that p is the data generating probability density, then a proper score S fulfills for any probability density q

$$\mathbb{E}_{Y \sim p}[S(p; Y)] \leq \mathbb{E}_{Y \sim p}[S(q; Y)]. \quad (22)$$

A score is strictly proper when equality in the above holds iff $q = p$ [Gneiting and Raftery, 2007].

Bröcker and Smith [2007] stress the importance of proper scoring rules for honest distributional forecasts. The NLL is a strictly proper scoring rule, which is why we use it in the present work. Strict propriety of the NLL can quickly be seen by plugging the NLL into the definition of a proper scoring rule and reducing it to the Kullback-Leibler divergence

$$\begin{aligned} \mathbb{E}_{Z \sim p}[-\log(q(Z))] &\geq \mathbb{E}_{Z \sim p}[-\log(p(Z))] \\ \Leftrightarrow \mathbb{E}_{Z \sim p}[-\log(q(Z))] - \mathbb{E}_{Z \sim p}[-\log(p(Z))] &\geq 0 \\ \Leftrightarrow \mathbb{E}_{Z \sim p}[\log(p(Z)/q(Z))] &= \text{KL}(p||q) \geq 0 \end{aligned} \quad (23)$$

which is indeed larger than 0 and equality holds iff $p = q$ [Kullback and Leibler, 1951]. Indeed, any affine transformation of the NLL is a strictly proper scoring rule, which follows directly from linearity of the expected value. An example would be a weighted NLL in which the weights are chosen inversely proportional to the frequency of the different outcome classes.

As noted in the main text, only the probability assigned to the true class enters the likelihood function. If a score is evaluated only at the observed outcome the score is called local. To use a non-local proper scoring rule alongside the local NLL that takes into account the whole predicted conditional distribution of an ordinal outcome we use the ranked probability score (RPS). The RPS is defined as

$$\text{RPS}(p; y) = \frac{1}{K-1} \sum_{k=1}^K \left(\sum_{j=1}^k p_j - \sum_{j=1}^k e_j \right)^2, \quad (24)$$

where K denotes the number of classes, p_j and e_j are the predicted and actual probability of class j , respectively. Note, that in most cases e_j is given by the j th entry of the one-hot encoded outcome. By summing over all K classes the RPS incorporates the whole predicted probability distribution and thus is a non-local scoring rule. The RPS is a proper scoring rule, which can be shown by reducing it to the sum of individual Brier scores at the classes $k = 1, \dots, K$. The Brier score is a proper score for binary outcomes and given by

$$\text{BS}(p; y) = (y - p)^2. \quad (25)$$

By introducing another predicted probability $q \in (0, 1)$, the expectation w.r.t. p can be written as

$$\mathbb{E}_{Y \sim p}[(Y - p)^2] = \mathbb{E}_{Y \sim p}[(Y - q + q - p)^2] = \mathbb{E}_{Y \sim p}[(Y - q)^2] - (p - q)^2. \quad (26)$$

where $(p - q)^2$ will always be positive and hence

$$\mathbb{E}_{Y \sim p}[(Y - p)^2] \leq \mathbb{E}_{Y \sim p}[(Y - q)^2] \quad (27)$$

which shows strict propriety of the Brier score. The last step is now to sum up the K individual Brier scores to arrive at the RPS. Because each Brier score is proper, the sum will also be minimal for the data generating distribution of the ordinal outcome. However, the RPS is not strictly proper because individual probabilities can be switched without changing the overall sum.

Some scoring rules possess a less desirable property in that they encourage overly confident predictions by assigning a too high probability to the predicted outcome value and thus fail to capture the actual uncertainty. Such a score is called improper and examples include the linear score and mean square error [Bröcker and Smith, 2007]. Although the accuracy is a commonly used metric, its use is neither recommended for assessing probabilistic predictions nor classification performance. This is because it is not a scoring rule and formulating it as one requires additional assumptions, which may very well yield an improper scoring rule [Harrell, 2020]. Also the QWK loss (see Appendix C),

$$\ell(p) = \log(1 - \kappa(p)), \quad (28)$$

as proposed by de La Torre et al. [2018] is improper. This can be seen by taking the data generating density of an ordinal random variable $Y \in \{y_1 < y_2 < y_3\}$ to be

$$p(y) = \begin{cases} 0.3 & \text{if } y = y_1, \\ 0.4 & \text{if } y = y_2, \\ 0.3 & \text{if } y = y_3; \end{cases}$$

for which the expected score will be

$$\mathbb{E}_p(\log(1 - \kappa(p))) = \sum_{k=1}^K p(y_k) \log(1 - \kappa(p)) = -0.693 \quad (29)$$

However, by forecasting a density q that puts more mass on p 's mode, $Y = y_2$,

$$q(y) = \begin{cases} 0.1 & \text{if } y = y_1, \\ 0.8 & \text{if } y = y_2, \\ 0.1 & \text{if } y = y_3; \end{cases} \quad (30)$$

we can achieve a much lower (better) score

$$\mathbb{E}_{Y \sim p}(\log(1 - \kappa(q))) = \sum_{k=1}^K p(y_k) \log(1 - \kappa(q)) = -1.386 \quad (31)$$

which proves impropriety of the QWK loss by counterexample. The same argument holds for $K = 2$ and $K > 3$, as well as different weighting schemes (no weighting, linear weights, higher order weights).

E Contrasting ordinal regression and classification

Here, we assess the benefit of using a proper versus an improper score for training and contrast ordinal regression (predicting a distribution) versus classification (predicting a single class or level). To this end, we compare ONTRAMs against a recently developed ordinal classifier, which uses the quadratic weighted kappa (QWK) loss [de La Torre et al., 2018] (see Appendix C). While the discussion so far was focusing on ordinal regression models, predicting a faithful conditional probability distribution, the developed (QWK-based) methods primarily aim for predicting the correct class and penalize misclassifications by their distance to the correct class. The QWK loss is an improper scoring rule and does not make an honest probabilistic prediction but encourages overly confident predictions (as we show in Appendix D). We emphasize the differences between taking a regression versus a classification approach to problems with an ordinal outcome. For that we use different performance measures to compare the MCC model for probabilistic multi-class classification, with the QWK model for ordinal classification and the CI ONTRAMs (CI_x for wine quality and CI_B for UTKFace in Figure E1). In (ordinal) classification tasks it is common to report the test accuracy and quadratic weighted kappa, although they are improper scoring rules (Appendix D).

While it is unfair by design to compare ordinal regression models trained with NLL loss, and ordinal classification models trained with a QWK loss, in terms of NLL or QWK-based evaluation metrics, such comparisons are commonly seen. The QWK model shows a strong performance deficit in terms of NLL and RPS compared to the MCC and CI models for all three datasets, because the QWK loss is improper (see Figure E1). Conversely, we observe a better continuous quadratic weighted kappa for the QWK model. These results are expected due to the different optimization criteria of the models but can be misleading at first sight. The discrete QWK metric shows almost on-par performance of all three models for the wine quality, while for the UTKFace data the QWK model performs worst.

Albeit not an ordinal evaluation metric we compare the models in terms of classification accuracy, as this is commonly done in benchmarking (ordinal) classification models. The accuracy is

misleading for various reasons. It is discontinuous at an implicitly used threshold probability and yields misleading results if classes are strongly unbalanced [see Appendix D and Harrell, 2020]. In the comparison in Figure E1 the QWK model shows the worst and the MCC model best accuracy closely followed by the CI ONTRAM for all three datasets. Both the theoretical considerations and the inconclusive results in Figure E1 indicate that it is advantageous to refrain from using classification accuracy to evaluate probabilistic regression or classification models.

Before closing this section, we want to stress the advantage of using proper scoring rules for assessing the prediction performance of an ordinal regression model that focuses on predicting a whole conditional distribution, embracing the uncertainty in the prediction. Also the MCC model is a probabilistic model and can therefore be assessed via proper scoring rules. Solely the QWK model is focusing on ordinal classification and therefore care should be taken when evaluating it with both proper and improper scoring rules and comparing it to ordinal regression models.

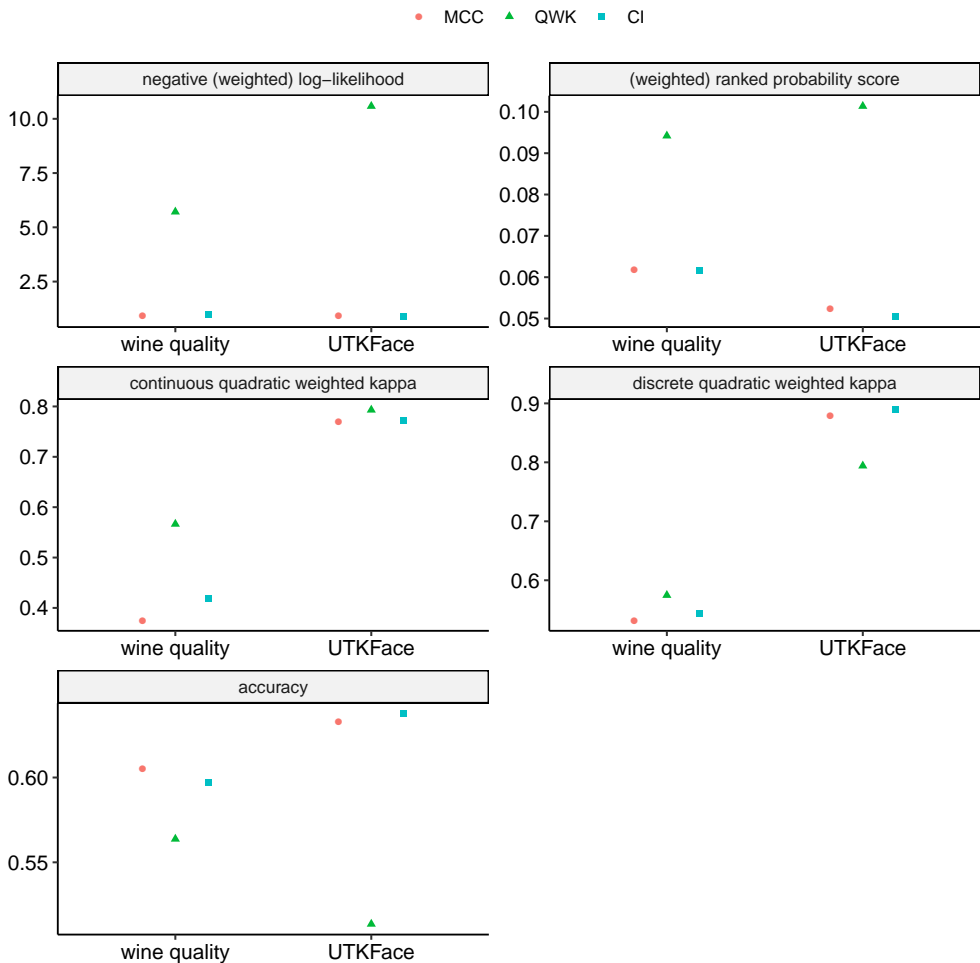


Figure E1: Test performance of the MCC model for probabilistic multi-class classification, the QWK model for ordinal classification and the CI (complex intercept) ONTRAM for ordinal regression in terms of NLL, RPS, continuous and discrete QWK, and accuracy for the wine quality and UTKFace datasets. The continuous QWK is obtained by back-transforming the QWK loss to its original scale via $1 - \exp(\ell(p))$.

F Confusion matrices and accuracy UTKFace

Example images of the ordered classes of the UTKFace data are given in Figure F1. UTKFace shows a moderately imbalanced marginal distribution of the class levels (7.99% baby, 6.41% child, 4.98% teenager, 34.04% young adult, 22.92% adult, 13.57% middle aged, 10.1% senior).

Table F1: Outcome distribution in the UTKFace test dataset stratified by sex.

	Age group						
Sex	[0, 4)	[4, 13)	[13, 20)	[20, 31)	[31, 46)	[46, 61)	[61, 117)
male	194	135	112	666	640	480	269
female	195	185	139	936	411	180	199



Figure F1: Example images for UTKFace. Example images of the seven classes (baby, child, teenager, young adult, adult, middle aged and senior) of the cropped and aligned UTKFace dataset are presented.

Figure F2 shows the confusion matrices for all fitted models. Class-wise accuracies are depicted in Figure F3.

The MCC and QWK models as well as the ONTRAMs yield similar confusion matrices and class-wise accuracies across all models.

		MCC							MCC-x							QWK						
predicted	[61, 117)	333	28	0	1	1	0	0	377	84	0	0	0	0	0	379	141	8	4	0	0	0
	[46, 61)	50	230	50	14	1	2	2	12	226	97	32	0	0	0	5	142	72	21	7	0	2
	[31, 46)	0	9	25	9	1	0	0	0	8	73	84	1	0	0	1	17	51	56	14	0	0
	[20, 31)	3	41	158	1315	425	49	6	0	2	81	1295	217	2	0	0	10	99	1137	304	36	6
	[13, 20)	1	6	14	251	549	268	42	0	0	0	185	640	91	0	4	10	21	384	726	624	460
	[4, 13)	0	4	2	11	70	298	167	0	0	0	6	188	389	47	0	0	0	0	0	0	0
	[0, 4)	2	2	2	1	4	43	251	0	0	0	0	5	178	421	0	0	0	0	0	0	0
			Cl _B							Cl _B -LS _x							SI-CS _B					
predicted	[61, 117)	364	45	1	1	0	0	0	361	67	0	0	0	0	0	368	99	2	0	0	0	0
	[46, 61)	19	208	48	18	2	1	1	27	215	29	2	0	0	0	9	93	11	2	0	0	0
	[31, 46)	0	19	43	23	3	0	0	1	24	83	39	0	0	0	0	0	0	0	0	0	0
	[20, 31)	3	39	147	1257	397	48	9	0	14	139	1378	224	2	0	10	123	226	1339	442	52	3
	[13, 20)	1	5	10	285	531	200	28	0	0	0	182	728	156	2	1	3	12	248	487	226	40
	[4, 13)	0	0	2	15	103	304	114	0	0	0	1	97	404	81	0	2	0	13	113	251	106
	[0, 4)	2	4	0	3	15	107	316	0	0	0	0	2	98	385	1	0	0	0	9	131	319
			SI-CS _B -LS _x							SI-LS _x												
predicted	[61, 117)	344	71	0	1	0	0	0	332	64	2	0	0	0	0							
	[46, 61)	43	197	39	2	0	0	0	54	199	42	5	0	0	0							
	[31, 46)	2	37	65	36	0	0	0	3	40	64	42	0	0	0							
	[20, 31)	0	15	147	1382	245	2	0	0	17	143	1349	264	2	0							
	[13, 20)	0	0	0	180	697	161	2	0	0	0	202	670	183	7							
	[4, 13)	0	0	0	1	109	398	95	0	0	0	4	116	375	105							
	[0, 4)	0	0	0	0	0	99	371	0	0	0	0	1	100	356							
		[0, 4)	[4, 13)	[13, 20)	[20, 31)	[31, 46)	[46, 61)	[61, 117)	[0, 4)	[4, 13)	[13, 20)	[20, 31)	[31, 46)	[46, 61)	[61, 117)	[0, 4)	[4, 13)	[13, 20)	[20, 31)	[31, 46)	[46, 61)	[61, 117)
		target																				

Figure F2: Confusion matrices for UTKFace data for all models mentioned in Table 1. The figure summarizes the true (x-axis) vs. the predicted (y-axis) classes for the fitted models. The predicted class is the class with the highest predicted probability.

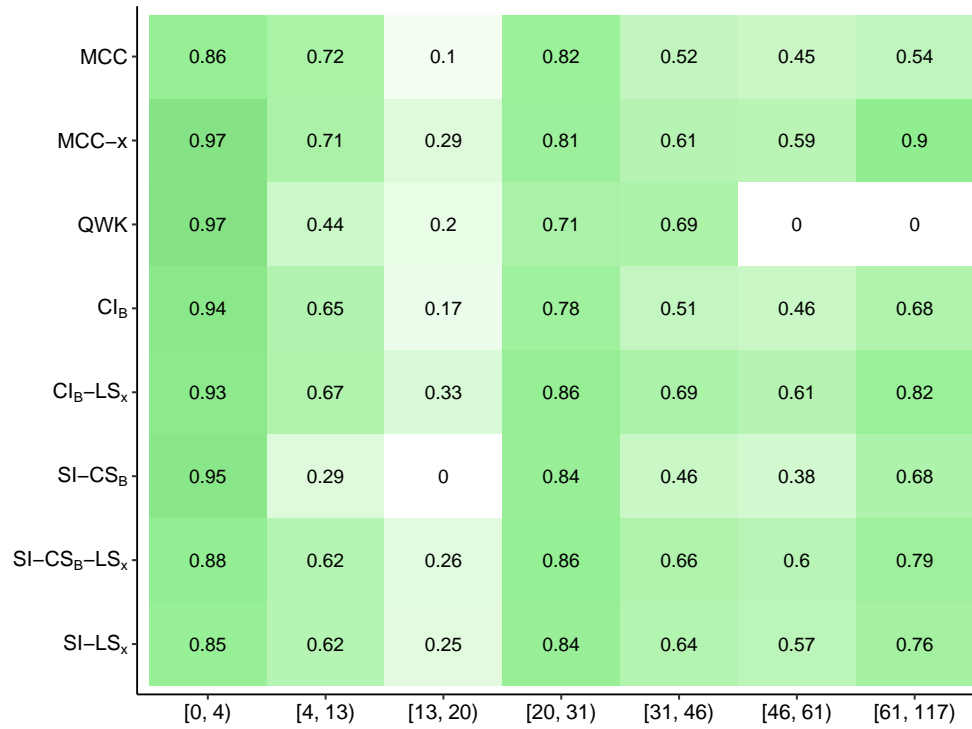


Figure F3: Class-wise accuracies of all models discussed in the main text for the UTKFace data.

References

- Martín Abadi et al. TensorFlow: Large-scale machine learning on heterogeneous systems, 2015. URL <http://tensorflow.org/>. Software available from tensorflow.org.
- Rishabh Agarwal, Nicholas Frosst, Xuezhou Zhang, Rich Caruana, and Geoffrey E Hinton. Neural additive models: Interpretable machine learning with neural nets. *arXiv preprint arXiv:2004.13912*, 2020.
- José P Amorim, Inês Domingues, Pedro Henriques Abreu, and João AM Santos. Interpreting deep learning models for ordinal problems. In *Proceedings of the European Symposium on Artificial Neural Networks*, 2018.
- Mikhail Belkin, Daniel Hsu, Siyuan Ma, and Soumik Mandal. Reconciling modern machine-learning practice and the classical bias–variance trade-off. *Proceedings of the National Academy of Sciences*, 116(32):15849–15854, 2019. doi: 10.1073/pnas.1903070116.
- Jochen Bröcker and Leonard A Smith. Scoring probabilistic forecasts: The importance of being proper. *Weather and Forecasting*, 22(2):382–388, 2007. doi: 10.1175/WAF966.1.
- Carol S Burckhardt and Kathryn L Anderson. The quality of life scale (QOLS): Reliability, validity, and utilization. *Health and Quality of Life Outcomes*, 1(1):60, 2003. doi: 10.1186/1477-7525-1-60.
- Muriel Buri and Torsten Hothorn. Model-based random forests for ordinal regression. *The International Journal of Biostatistics*, 1(ahead-of-print), 2020. doi: 10.1515/ijb-2019-0063.
- Wenzhi Cao, Vahid Mirjalili, and Sebastian Raschka. Rank-consistent ordinal regression for neural networks. *arXiv preprint arXiv:1901.07884*, 2019.
- Jaime S Cardoso and Joaquim F Costa. Learning to classify ordinal data: The data replication method. *Journal of Machine Learning Research*, 8(Jul):1393–1429, 2007. URL <https://www.jmlr.org/papers/v8/cardoso07a.html>.
- Jianlin Cheng, Zheng Wang, and Gianluca Pollastri. A neural network approach to ordinal regression. In *2008 IEEE International Joint Conference on Neural Networks (IEEE World Congress on Computational Intelligence)*, pages 1279–1284. IEEE, 2008. doi: 10.1109/IJCNN.2008.4633963.
- François Chollet et al. Keras. <https://keras.io>, 2015.
- Rune Haubo Bojesen Christensen. *ordinal: Regression Models for Ordinal Data*, 2019. URL <https://CRAN.R-project.org/package=ordinal>. R package version 2019.12-10.
- Wei Chu and Zoubin Ghahramani. Gaussian processes for ordinal regression. *Journal of Machine Learning Research*, 6(Jul):1019–1041, 2005. URL <https://www.jmlr.org/papers/v6/chu05a.html>.
- Wei Chu and S Sathiya Keerthi. Support vector ordinal regression. *Neural Computation*, 19(3):792–815, 2007. doi: 10.1162/neco.2007.19.3.792.
- Jacob Cohen. A coefficient of agreement for nominal scales. *Educational and Psychological Measurement*, 20(1):37–46, 1960. doi: 10.1177/001316446002000104.
- Jacob Cohen. Weighted kappa: nominal scale agreement provision for scaled disagreement or partial credit. *Psychological Bulletin*, 70(4):213, 1968. doi: 10.1037/h0026256.

- Jacob Cohen. A power primer. *Psychological Bulletin*, 112(1):155, 1992. doi: 10.1037/0033-2909.112.1.155.
- David Collett. *Modelling survival data in medical research*. CRC press, 2015.
- Paulo Cortez, António Cerdeira, Fernando Almeida, Telmo Matos, and José Reis. Modeling wine preferences by data mining from physicochemical properties. *Decision Support Systems*, 47(4): 547–553, 2009. doi: 10.1016/j.dss.2009.05.016.
- Jordi de La Torre, Domenec Puig, and Aida Valls. Weighted kappa loss function for multi-class classification of ordinal data in deep learning. *Pattern Recognition Letters*, 105:144–154, 2018. doi: 10.1016/j.patrec.2017.05.018.
- Jordi de La Torre, Aida Valls, and Domenec Puig. A deep learning interpretable classifier for diabetic retinopathy disease grading. *Neurocomputing*, 396:465–476, 2020.
- Eibe Frank and Mark Hall. A simple approach to ordinal classification. In *European Conference on Machine Learning*, pages 145–156. Springer, 2001. doi: 10.1007/3-540-44795-4_13.
- Yarin Gal and Zoubin Ghahramani. Dropout as a Bayesian approximation: Representing model uncertainty in deep learning. In *International Conference on Machine Learning*, pages 1050–1059, 2016.
- Bhanu Garg and Naresh Manwani. Robust deep ordinal regression under label noise. *arXiv preprint arXiv:1912.03488*, 2019.
- Frederic C Genter and Vernon T Farewell. Goodness-of-link testing in ordinal regression models. *Canadian Journal of Statistics*, 13(1):37–44, 1985. doi: 10.2307/3315165.
- Tilmann Gneiting and Adrian E Raftery. Weather forecasting with ensemble methods. *Science*, 310(5746):248–249, 2005. doi: 10.1126/science.1115255.
- Tilmann Gneiting and Adrian E Raftery. Strictly proper scoring rules, prediction, and estimation. *Journal of the American Statistical Association*, 102(477):359–378, 2007. doi: 10.1198/016214506000001437.
- Ian Goodfellow, Yoshua Bengio, and Aaron Courville. *Deep learning*. MIT press, 2016. doi: 10.1007/s10710-017-9314-z.
- Frank Harrell. Biostatistics for biomedical research, 2020. URL <http://hbiostat.org/doc/bbr.pdf>.
- Trevor J Hastie and Robert J Tibshirani. *Generalized additive models*, volume 43. CRC press, 1990. doi: 10.1002/9781118445112.stat03141.
- Torsten Hothorn. Transformation boosting machines. *Statistics and Computing*, 30(1):141–152, 2020a. doi: 10.1007/s11222-019-09870-4.
- Torsten Hothorn. *tram: Transformation Models*, 2020b. URL <https://CRAN.R-project.org/package=tram>. R package version 0.5-1.
- Torsten Hothorn and Achim Zeileis. Transformation forests. *arXiv preprint arXiv:1701.02110*, 2017.

- Torsten Hothorn, Peter Bühlmann, Thomas Kneib, Matthias Schmid, and Benjamin Hofner. Model-based boosting 2.0. *Journal of Machine Learning Research*, 11:2109–2113, 2010. URL <http://jmlr.org/papers/v11/hothorn10a.html>.
- Torsten Hothorn, Thomas Kneib, and Peter Bühlmann. Conditional transformation models. *Journal of the Royal Statistical Society: Series B: Statistical Methodology*, pages 3–27, 2014. doi: 10.1111/rssb.12017.
- Solomon Kullback and Richard A Leibler. On information and sufficiency. *The Annals of Mathematical Statistics*, 22(1):79–86, 1951. doi: 10.1214/aoms/1177729694.
- Balaji Lakshminarayanan, Alexander Pritzel, and Charles Blundell. Simple and scalable predictive uncertainty estimation using deep ensembles. In *Advances in Neural Information Processing Systems*, pages 6402–6413, 2017.
- Yanzhu Liu, Adams Wai-Kin Kong, and Chi Keong Goh. Deep ordinal regression based on data relationship for small datasets. In *Proceedings of the International Joint Conference on Artificial Intelligence*, pages 2372–2378, 2017. doi: 10.24963/ijcai.2017/330.
- Yanzhu Liu, Fan Wang, and Adams Wai Kin Kong. Probabilistic deep ordinal regression based on gaussian processes. In *Proceedings of the IEEE International Conference on Computer Vision*, pages 5301–5309, 2019. doi: 10.1109/ICCV.2019.00540.
- Charles F Manski and Steven R Lerman. The estimation of choice probabilities from choice based samples. *Econometrica: Journal of the Econometric Society*, pages 1977–1988, 1977.
- Peter McCullagh. Regression models for ordinal data. *Journal of the Royal Statistical Society: Series B (Methodological)*, 42(2):109–127, 1980. doi: 10.1111/j.2517-6161.1980.tb01109.x.
- Zhenxing Niu, Mo Zhou, Le Wang, Xinbo Gao, and Gang Hua. Ordinal regression with multiple output cnn for age estimation. In *Proceedings of the IEEE Conference on Computer Vision and Pattern Recognition*, pages 4920–4928, 2016. doi: 10.1109/CVPR.2016.532.
- M Opper, W Kinzel, J Kleinz, and R Nehl. On the ability of the optimal perceptron to generalise. *Journal of Physics A: Mathematical and General*, 23(11):L581, 1990. doi: 10.1088/0305-4470/23/11/012.
- Harry Pratt, Frans Coenen, Deborah M Broadbent, Simon P Harding, and Yalin Zheng. Convolutional neural networks for diabetic retinopathy. *Procedia Computer Science*, 90:200–205, 2016. doi: 10.1016/j.procs.2016.07.014.
- R Core Team. *R: A Language and Environment for Statistical Computing*. R Foundation for Statistical Computing, Vienna, Austria, 2020. URL <https://www.R-project.org/>.
- Marco Tulio Ribeiro, Sameer Singh, and Carlos Guestrin. “Why should I trust you?” explaining the predictions of any classifier. In *Proceedings of the 22nd ACM SIGKDD International Conference on Knowledge Discovery and Data Mining*, pages 1135–1144, 2016.
- Janick Rohrbach, Tobias Reinhard, Beate Sick, and Oliver Dürr. Bone erosion scoring for rheumatoid arthritis with deep convolutional neural networks. *Computers & Electrical Engineering*, 78: 472–481, 2019. doi: 10.1016/j.compeleceng.2019.08.003.

- Javier Sánchez-Monedero, Pedro Antonio Gutiérrez, and María Pérez-Ortiz. ORCA: A Matlab/Octave toolbox for ordinal regression. *Journal of Machine Learning Research*, 20, 2019. URL <https://www.jmlr.org/papers/v20/18-349.html>.
- Beate Sick, Torsten Hothorn, and Oliver Dürr. Deep transformation models: Tackling complex regression problems with neural network based transformation models. *arXiv preprint arXiv:2004.00464*, 2020.
- Sandra Siegfried and Torsten Hothorn. Count transformation models. *Methods in Ecology and Evolution*, 11(7):818–827, 2020. doi: 10.1111/2041-210X.13383.
- Karen Simonyan and Andrew Zisserman. Very deep convolutional networks for large-scale image recognition. *arXiv:1409.1556*, 09 2014.
- Nitish Srivastava, Geoffrey Hinton, Alex Krizhevsky, Ilya Sutskever, and Ruslan Salakhutdinov. Dropout: A simple way to prevent neural networks from overfitting. *Journal of Machine Learning Research*, 15:1929–1958, 2014. URL <http://jmlr.org/papers/v15/srivastava14a.html>.
- Gerhard Tutz. *Regression for categorical data*, volume 34. Cambridge University Press, 2011. doi: 10.1017/CBO9780511842061.
- Guido Van Rossum and Fred L Drake Jr. *Python reference manual*. Centrum voor Wiskunde en Informatica Amsterdam, 1995.
- Víctor Manuel Vargas, Pedro Antonio Gutiérrez, and César Hervás. Deep ordinal classification based on the proportional odds model. In *International Work-Conference on the Interplay Between Natural and Artificial Computation*, pages 441–451. Springer, 2019. doi: 10.1109/BTAS.2016.7791154.
- Víctor Manuel Vargas, Pedro Antonio Gutiérrez, and César Hervás-Martínez. Cumulative link models for deep ordinal classification. *Neurocomputing*, 2020. doi: 10.1016/j.neucom.2020.03.034.
- Andrew Gordon Wilson and Pavel Izmailov. Bayesian deep learning and a probabilistic perspective of generalization. *arXiv preprint arXiv:2002.08791*, 2020.
- Simon N Wood. *Generalized Additive Models: An Introduction with R*. Chapman and Hall/CRC, 2 edition, 2017.
- Haiping Zhu, Qi Zhou, Junping Zhang, and James Z Wang. Facial aging and rejuvenation by conditional multi-adversarial autoencoder with ordinal regression. *arXiv preprint arXiv:1804.02740*, 2018.
- Haiping Zhu, Yuheng Zhang, Guohao Li, Junping Zhang, and Hongming Shan. Ordinal distribution regression for gait-based age estimation. *Science China Information Sciences*, 63(2):120102, 2020. doi: 10.1007/s11432-019-2733-4.